QA: N/A

MOL.20010725.0121

Long-Term Degradation of Concrete Facilities Presently Used for Storage of Spent Nuclear Fuel and High-Level Waste

Revision 1
October 1998

Prepared for Jason Technologies
6655 West Sahara Avenue
Las Vegas, NV 89102

Report Prepared for Use in Preparation of the Yucca Mountain Environmental Impact Statement

Report by: W. Lee Poe, Jr.
Tetra Tech NUS, Inc.
900 Trail Ridge Road
Aiken, SC 29803

TABLE OF CONTENTS

TABLE OF CONTENTS (Continued

List of Tables

List of Figures

TABLE OF CONTENTS (Continued)

BACKGROUND AND ANALYSIS SUMMARY

S.1 Purpose and Background

This paper is intended to describe aging of concrete and its application to the Yucca Mountain Environmental Impact Statement (YM EIS) No-Action Alternatives. Concrete structures are considered to be the most probable outer engineered barrier for the spent nuclear fuel (SNF) and high-level waste (HLW). The document does not evaluate other engineered barriers that must also be breached before release of materials from the SNF or HLW can affect the environment. Later analyses will be developed to evaluate their failure and then composite failure identified and quantified.

Concrete barriers were never intended for long term storage of SNF or HLW. Most have design lives of about 50 years but many concrete-like structures have survived for centuries. The information presented in this paper should serve as a tool to select one of the assumptions necessary for evaluation of the No-Action Alternative environmental evaluation.

S.2 Report Content

This document contains (1) a general description of existing or planned concrete storage facilities used to store the SNF and HLW, (2) a section on concrete aging and breakdown mechanisms, (3) a summary of previous performance assessments reflecting conclusions on concrete facilities failure that may be applicable to the No-Action scenario, and (4) a proposed failure sequence recommendation for concrete structures used in the YM EIS.

The process provides an engineering and scientific basis for the assumptions made for analysis of the No-Action Alternatives.

S.3 Failure Scenario Conclusions

S.3.1 SURFACE CONCRETE STRUCTURES

Above-ground concrete structures are expected to degrade slowly over a period of time and expose their contents to conditions that may cause deterioration of the package contained within the concrete structure and the waste form. Although degradation of concrete is complex and caused by a number of mechanisms, one of the predominant mechanisms is freeze/thaw damage. Analysis of NUHOMS dry storage casks shows they may fail after 80 to 200 years if they are not maintained and result in loss of weather protection. The earliest failure time was determined for cold climates such as Saint Cloud, MN. The later failure time was for more moderate weather such as encountered in Augusta, GA. The freeze/thaw damage to concrete in Florida and California and other warm regions of the county is minimal and other degradation mechanisms apply.

S.3.2 UNDERGROUND CONCRETE STRUCTURES

Underground concrete structures are expected to last longer because they are in a more benign environment. For example, the Glass Waste Storage Facility at Savannah River Site (SRS) near Augusta, GA was evaluated, and the concrete within it was found to last about 3,000 years. However, the expected failure sequence for that facility may not be concrete failure. The weather protection portion of that facility (i.e., the roof) should protect its contents for 150 years until that cover is lost. At that time, the contents of the vault (in this case the High-Level Waste as a borosilicate glass in a stainless steel canister) will be exposed to precipitation. From 150 to 1,600 years the concrete vault is expected to serve as a tub, and the engineered barrier of the canister and leach resistance of the glass must provide protection. (The protection provided by the waste canister and the waste itself are not included in this analysis.) The failure consequence is also related to expected environmental conditions such as precipitation. The primary analyses included in Section 4 is for SRS environment which is a humid-mesic environment. Section 4 also gives an analysis for Hanford's arid-xeric environment. At 1,600 years the porosity of the concrete walls and floor will have increased because of concrete degradation and will leak to the vadose zone.

CHAPTER 1. GENERIC STRUCTURE DESCRIPTION CONSIDERED IN THE YUCCA MOUNTAIN EIS

The Yucca Mountain Environmental Impact Statement (YM EIS) No-Action Alternative must analyze the impacts of leaving the spent nuclear fuel (SNF) and high-level waste (HLW), evaluated in the Action Alternatives, at the generating sites for the 10,000-year-period evaluated in the Action Alternatives. This document considers the failure mechanism associated with the outer engineered barrier - the concrete housing. The barrier is basically the reinforced-concrete structures used to contain the SNF and HLW awaiting shipment to Yucca Mountain Repository. It assumes that institutional control is maintained for the first 100 years (from 2005, in the event that a flaw in the geologic repository is discovered and the license for the repository is not received from the NRC for operation of the repository) until 2105.

In looking at the various types of interim storage currently used or planned by the utilities and DOE generator sites, two generic types of facilities emerge: surface and underground concrete structures. An assumed typical example of each is (1) **surface storage** of light water SNF at utility sites in concrete casks and (2) **underground storage** of vitrified HLW in stainless steel canisters as is being used by DOE at SRS.

To illustrate these concepts, two specific designs were selected that are similar to those found in the YM EIS data call. They are:

- Surface Storage. NUHOMS® type horizontal storage module (HSM) used by several utilities to dry store their SNF until it is shipped to the geologic repository.

- Underground Storage. SRS Glass Storage Building used by DOE to store vitrified HLW at SRS until it is shipped to the geology repository.

Typical information is provided in the following two subsections.

1.1 NUHOMS Dry Shielded Canister System

This brief description of the NUHOMS Independent Spent Fuel Storage Installation (ISFSI) is based upon information obtained from References 1.1 and 1.2. Reference 1.1 was reviewed and accepted by NRC, and Reference 1.2 is the resulting safety evaluation report (SER). This section presents a brief summary of the design of the storage mode consisting of a concrete cask called an HSM, designed for storage on a concrete pad at the ground surface. Figure 1-1 shows a cut-away view of the HSM. Figure 1-2 shows a stylized plat used for storing 20 HSM with about 226 metric tons uranium (MTU) of SNF. These HMSs are designed for natural circulation of air for cooling the SNF. Either pressurized water reactor (PWR) or boiling water reactor (BWR) SNF is loaded into a dry shielded canister (DSC) and placed within the HSM for storage.

Safe storage of irradiated fuel is provided by a combination of the DSC and HSM, which provide shielding to ensure that any nearby persons or animals are protected from the penetrating radiation from the SNF. The DSC provides confinement of radioactive material. The HSM, a reinforced concrete structure, provides projectile impact and weather protection for the DSC and serves as the primary biological shield for the irradiated fuel during storage.

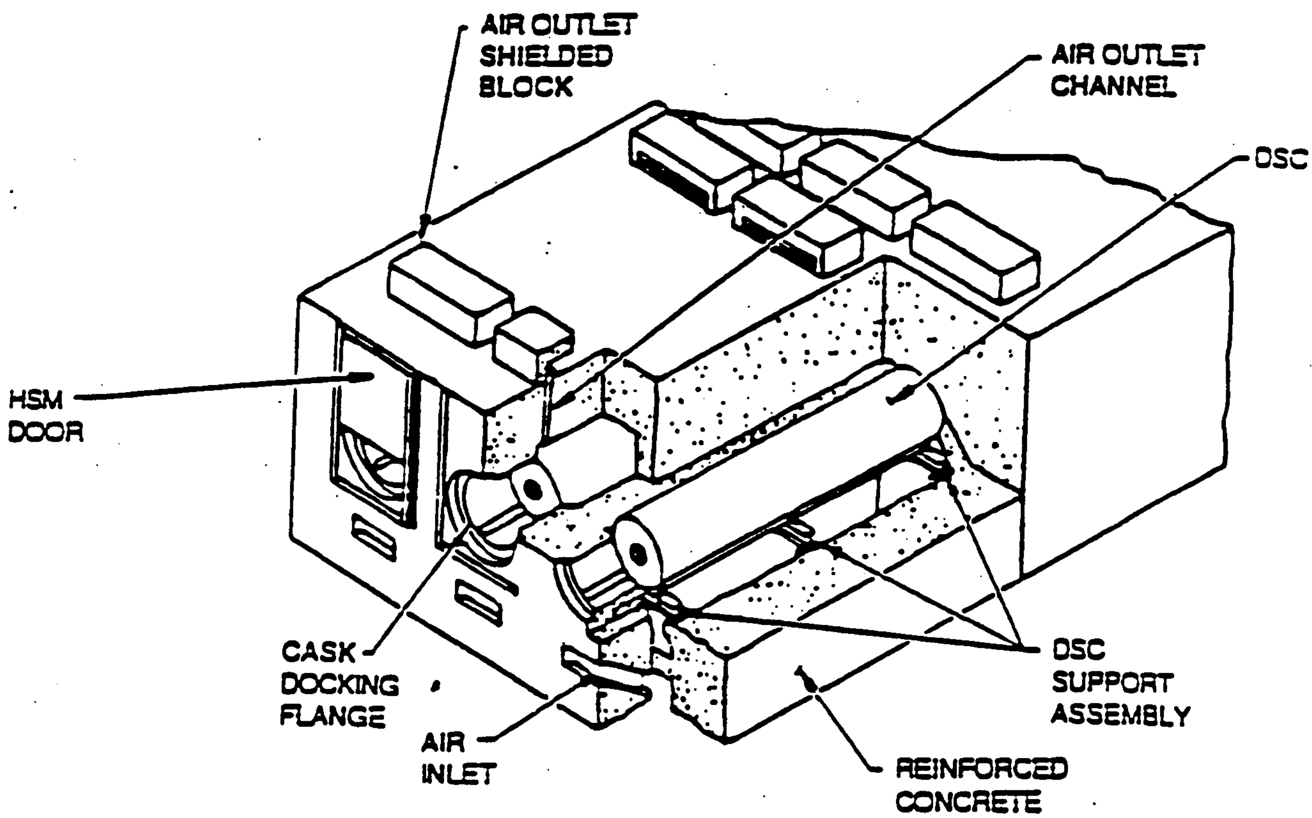

ARRAY OF TWO TO TWENTY HSMs

Figure 1-1. Interconntected HSMs.

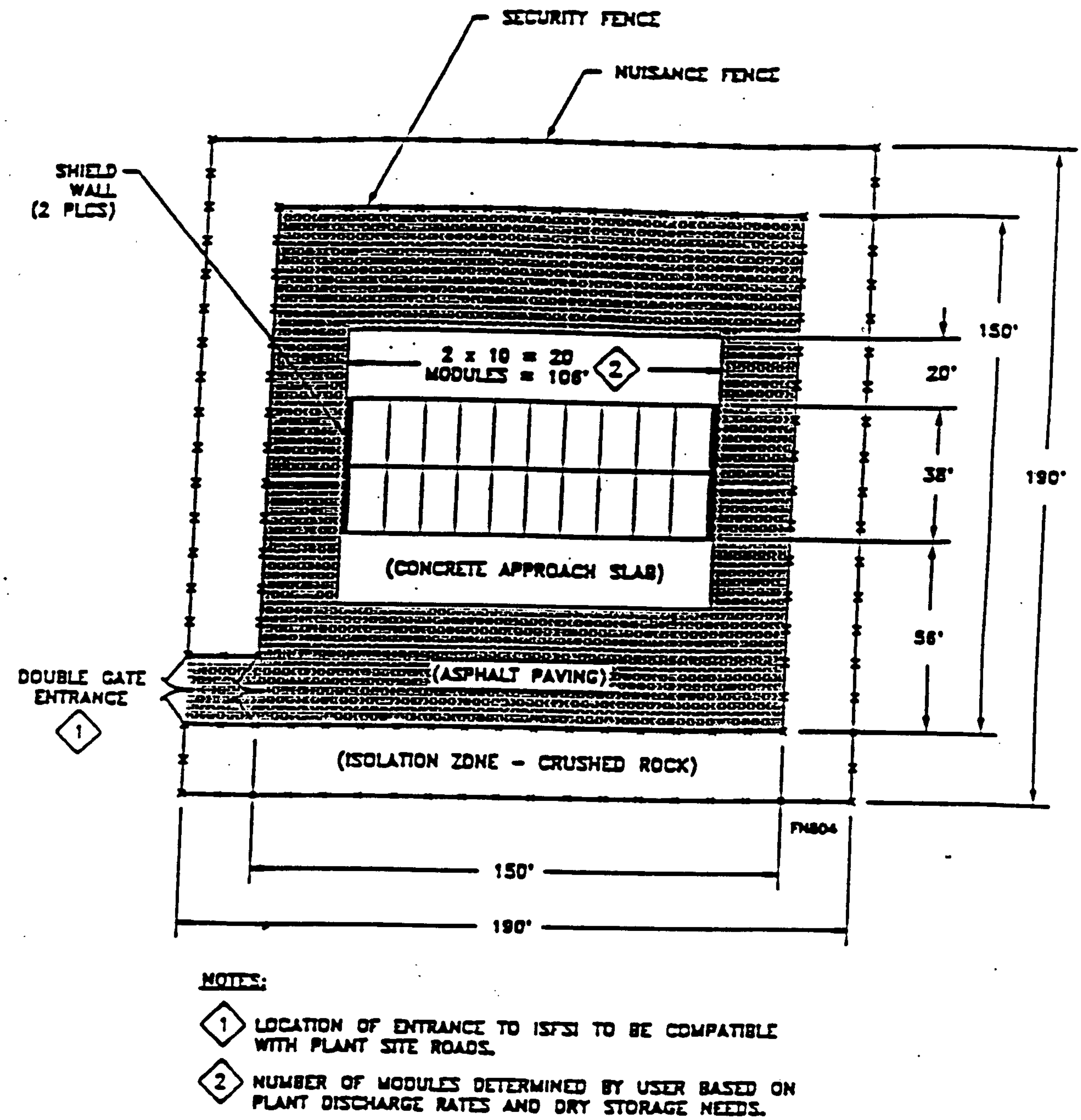

Figure 1-2. Standard double module row NUHOMS ISFSI layout.

The DSC (see Figure 1-3) shell is constructed of 0.625-inch-thick Type 304 stainless steel with all welded construction. These welds are fully radiographed and inspected according to the requirements of the ASME Boiler and Pressure Valve (B&PV) Code Section III, Division I, Subsection NB. The bottom end sandwiches lead between an outer plate and an inner plate of Type 304 stainless steel. The bottom end plug also includes a grapple attachment assembly for insertion and removal from the HSM. The top plug is formed by two covers, separately welded to the DSC shell. The inner cover and the outer cover are manufactured from Type 304 stainless steel with lead placed between these cover plates. The DSC is welded shut with an internal pressure of helium gas. The welds are multiple pass and are to be tested either ultrasonically or by multi-level dye penetration examination. In addition, a helium leak test will be performed after welding the inner top cover in place. The DSC end plugs and the canister shell provide confinement and radiation shielding.

The canister encloses a basket assembly, which can house 24 irradiated PWR fuel assemblies or 52 BWR fuel assemblies. The basket consists of eight spacer discs of Type 304 stainless steel that are fixed in the canister. There are 24 square section guide sleeves of Type 304 stainless steel that house the spent assemblies. The spacer discs and axial support rods maintain dimensional stability for the guide sleeves that house the SNF in the event of a vertical or horizontal drop. Figure 1-4 provides two cross sectional views of the HSM.

The HSM is designed to be constructed of 5,000 psi (minimum specified compressive strength) normal weight (145 pounds per cubic foot minimum density) concrete. The concrete is made with Type II Portland cement meeting the requirements of ASTM C150. The aggregate is to meet the specifications of the ASTM C33. The reinforcing steel is #10 bars ASTM A615 Grade 60 spaced 6 inches on centers each way each face, top, sides, front, back, and foundation.

The HSM wall thickness, which varies from 2 to 3 feet, was designed to meet shielding requirements and was checked against structural criteria. The walls protect the DSC against tornado-generated missiles, which effectively bounds reasonable impact accidents, as well as other environmental conditions, natural phenomena, and accidents.

The NUHOMS DSC is designed to provide nuclear criticality safety during wet loading and unloading operations. The moderator density conditions are an important factor for criticality safety during fuel loading into the DSC and if removal of fuel assemblies from the DSC is necessary for any reason. The DSC is initially filled with borated water ($\geq$ 1,810 ppm boron) prior to placement in the spent fuel pool, which is also borated. The loaded DSC is removed from the fuel pool and the DSC cavity is subsequently dried and backfilled with helium as part of the DSC closure operation. Flow paths are provided in the DSC design to ensure that the DSC draining or refilling process is a controlled process.

After fuel loading and DSC drying, the irradiated assemblies are not moderated during the design life of the DSC; therefore, criticality safety is assured during these subsequent operations and storage. During transfer and storage of the canistered SNF, ingress of water into the helium-filled DSC is precluded by its welded seals and its approval of the use of this design to storage on flood-free sites, eliminating water intrusion into the DSC as a credible event during the design life of this system (50 years). During the No-Action scenario, if the DSC containment fails and water seeps into the DSC, nuclear criticality must be considered.

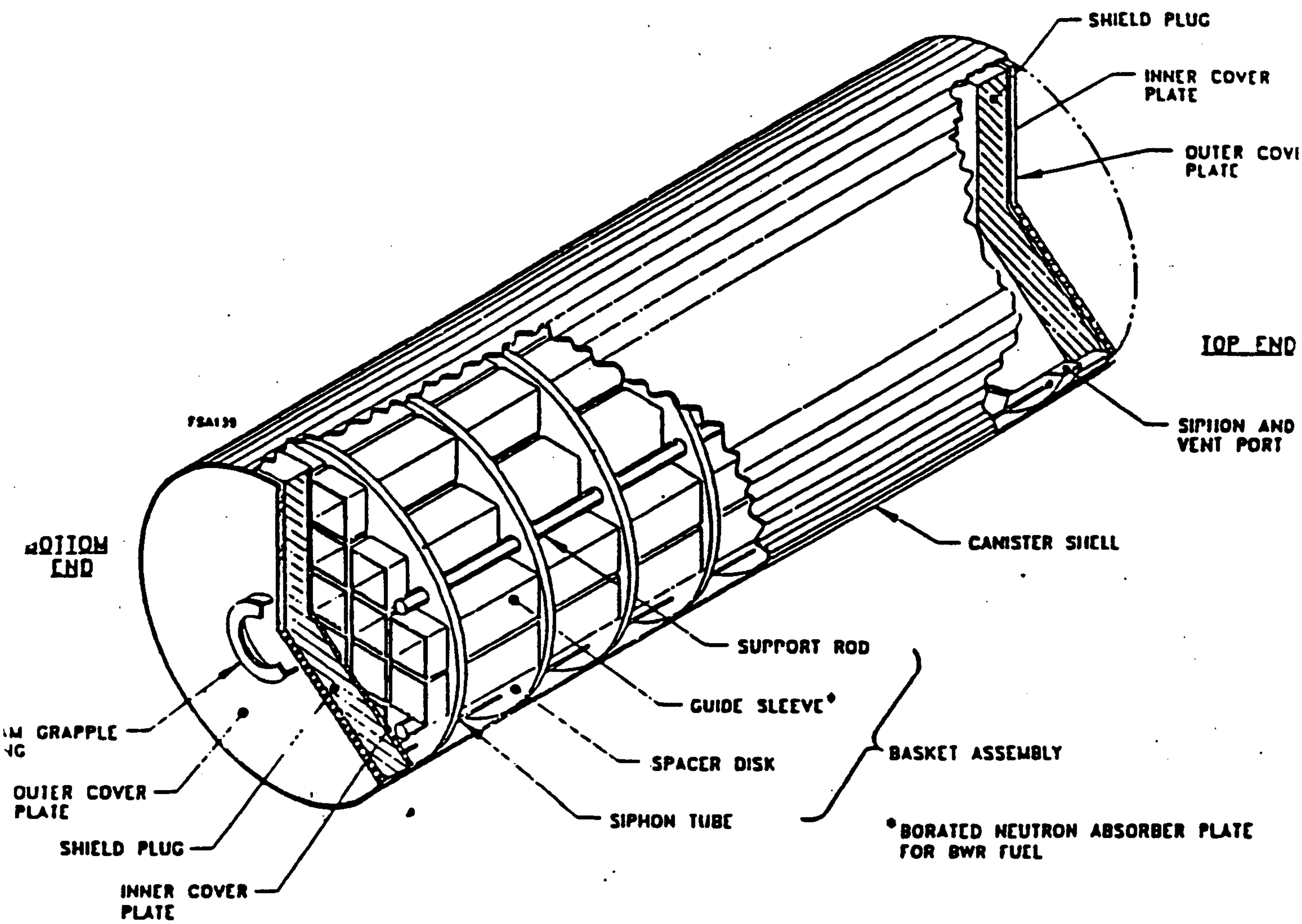

Figure 1-3. NUHOMS® dry shielded canister assembly components.

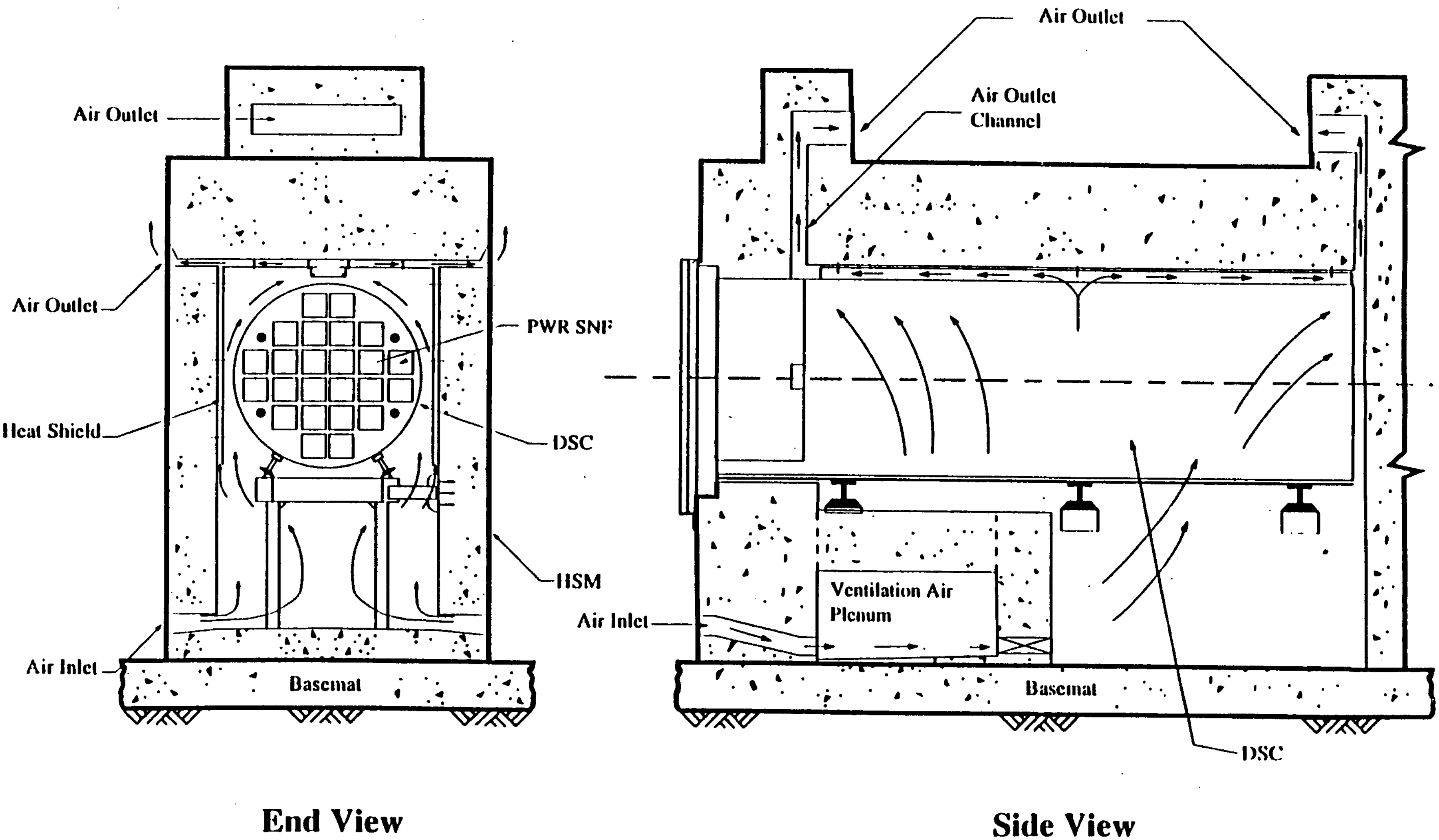

Figure 1-4. Cross section views of NUHOMS HSM.

Other ISFSIs are being used or are being discussed for storage of commercial SNF. They include vertical SNF storage in concrete casks and in modular concrete storage vaults. These storage concepts are located on the ground surface and incorporate concrete shielding to protect the surrounding environmental from penetrating radiation from the SNF. Most utilize dry storage of the SNF and passive cooling to prevent SNF from becoming overheated. In addition, the SNF is protected from the weather. In an earlier search for a single concept for analysis of the storage concept degradation, the NUHOMS concept was identified as the most likely form of storage for most of the commercial SNF.

1.2 Savannah River Site Glass Waste Storage Building (GWSB)

Vitrified HLW glass is cast into a 3/8 thick 304 stainless steel canister, the canisters are welded shut and decontaminated, the canisters are delivered to the Glass Waste Storage Building (GWSB) in a shielded canister transporter (SCT), and the canisters are stored in the GWSB (Ref. 1.3). The present GWSB has capacity for 2,286 canisters and is designed for expansion by construction of additional buildings (Ref. 1.4). It is expected that SRS will have three GWSBs to house the vitrified HLW glass until it is shipped to the geologic repository. The existing GWSB consists of four major areas including storage vaults, an operating area above the vault, air inlet shafts, and air exhaust shafts.

Upon entering the building at grade, the operator of the SCT locates the desired storage cavity. The SCT is positioned over the desired storage spot, the operating floor plug is removed, the glass waste canister is lowered into the storage vault, and the operating floor plug is replaced. The canisters are maintained in a vertical position by large diameter pipe sections that serve as vertical storage cavities, which are constructed of galvanized steel. The standard openings are laid out in a grid pattern, and the canister casings are supported by a concrete base mat. Space between the pipes is covered with overlapping horizontally stepped steel plates to direct most of the ventilation air through the storage pipes. The operating floor area of the GWSB is column free to allow clear access for the SCT to all the storage locations.

The canister storage vaults are located below the operating floor, which is slightly above grade. It is constructed to be earthquake- and tornado-resistant. Exterior damp-proofing is provided below grade. Figure 1-5 shows a simplified section of the facility. The vault area is designated to hold the radioactive glass waste canisters underground and protect operating personnel, the public, and the environment. Radiation shielding protection is provided by 34-inch thick reinforced concrete walls, earth embedment, and a concrete deck that forms the floor of the operating area. All canister storage locations will have individual precast concrete plugs. The 42-inch thick reinforced concrete floor is treated to resist powdering or spalling due to movement of the SCT. There are 2,262 standard and 24 oversize plug openings in the floor. Each plug must be easily removed and reinstalled but must have a tight fit. The operating floor and the storage vault is designed to support the SCT which weighs in excess of 260,000 pounds with a wheel load of approximately 135 pounds per square inch.

The storage vault, which has below-grade air shafts, is located underground and is constructed as a reinforced concrete box structure. For confinement purposes, the storage vault area is divided into independent vaults. Two vaults will form a module. Each vault has an air inlet, air exhaust, and air passage cell to house the canister supports.

Radioactive decay heat from around the canisters is removed by the building's forced air exhaust system. The exhaust air passes through the building's HEPA filter ventilation system and then discharged to the

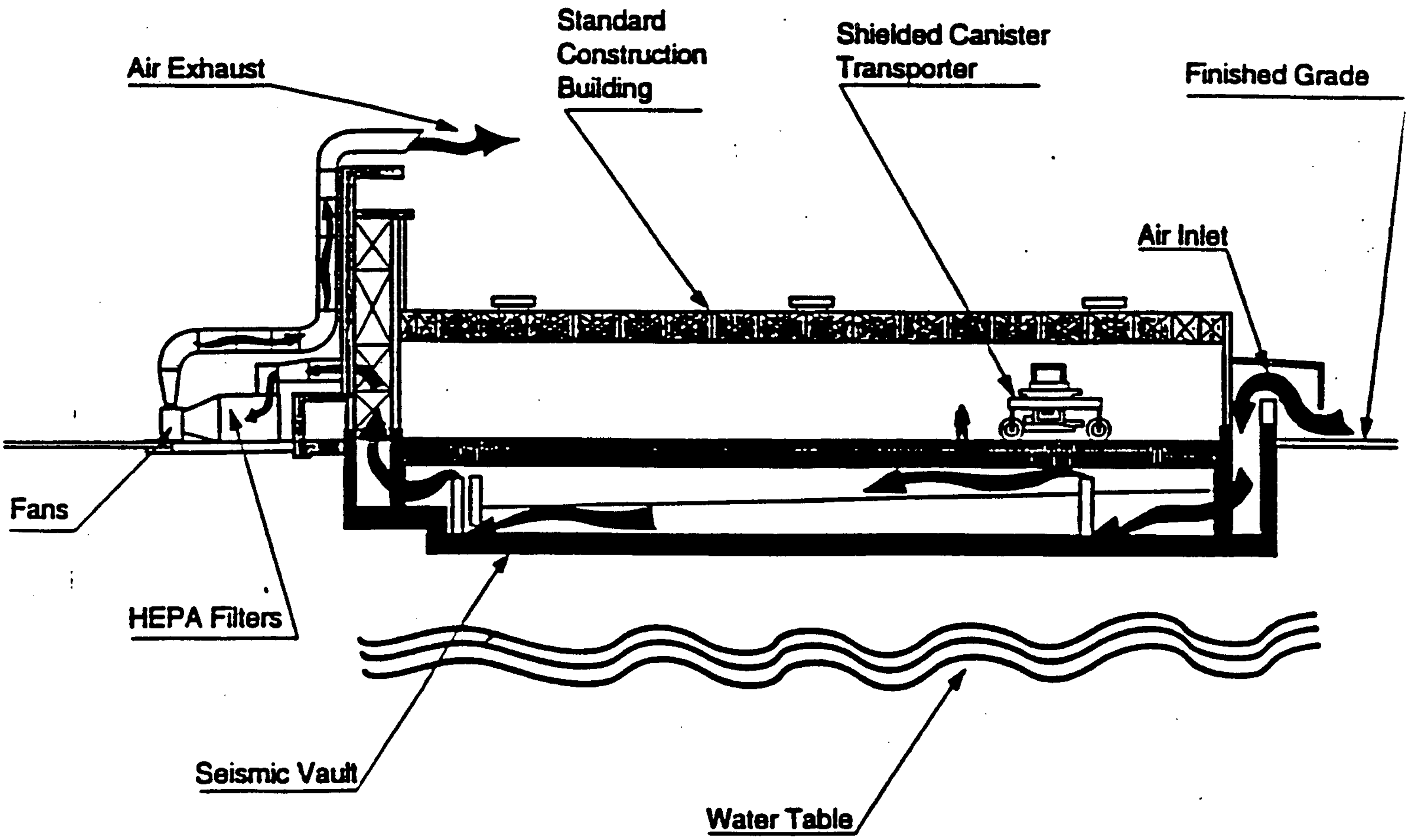

Figure 1-5. Glass waste storage building cross section.

atmosphere through a stack attached to the building. The storage vault is divided into four separate compartments for ventilation. Supply air is distributed across the bottom of each compartment. The oversize diameter of each pipe storage cavity allows air passage through the annular space around each stored waste canister. The exhaust air will be monitored for radioactivity using continuous air samplers during the loading and probably during building surveillance.

The SCT operating area above the vault is enclosed in a Category III (as defined by DOE Order 6430) steel structure. It has uninsulated metal siding and an insulated roof.

Any accumulated water inside a vault will be collected in stainless steel sumps (minimum of two in each vault) and the liquid level monitored. The water will be sampled for radioactive contamination and later pumped out of the vault using a portable sump pump; it is trucked to a waste management area for disposition.

1.3 Section 1 References

1.1 NUTEC, Inc., 1989, *Topical Report for the NUTEC Horizontal Modular Storage System for Irradiated Nuclear Fuel, NUHOMS-24*, NUH-002, Revision 1, July.

1.2 NRC (U.S. Nuclear Regulatory Commission), 1989, *Safety Evaluation Report Related to the NUTEC Horizontal Modular Storage System for Irradiated Nuclear Fuels, NUHOMS-24P*, NUH-002, April.

1.3 WSRC (Westinghouse Savannah River Company), 1997, *S-Area Defense Waste Processing Facility (S-Area DWPF) Final Safety Analysis Report*, WSRC-SA-6, March.

1.4 WSRC (Westinghouse Savannah River Company), 1992, *Project S-2045 - Glass Waste Storage Building #2*, WSRC-TR-90-570-002, Revision 1, March 31.

CHAPTER 2. DEGRADATION MECHANISMS FOR CONCRETE AND REINFORCING STEEL

(Adapted from BNL 52527, Ref. 2.1)

The age-related mechanisms that may affect concrete and reinforcing steel used in long-term storage of HLW and SNF are identified from a review and evaluation of their expected operating history, relevant laboratory test data, analytical assessments, and related experience with similar structures in other industries. The potential age-related degradation mechanisms are listed in Table 2-1.

Table 2-1. Possible degradation mechanisms for HLW and SNF storage in No-Action scenario.

Component	Mechanism
Potentially significant mechanisms	1. Elevated temperature
	2. Freezing and thawing
	3. Leaching of calcium hydroxide or other soluble constituents
Potentially non-significant mechanisms	4. Aggressive chemical/sulfate attack
	5. Alkali-aggregate reactions
	6. Creep and shrinkage
	7. Abrasion and cavitation
	8. Irradiation

The description below provides a general analysis of these degradation mechanisms with regard to the No-Action Alternative. Past studies (Ref. 2.1) have classified the degradation mechanisms into non-significant, potentially non-significant, and potentially significant. In this reference, a degradation mechanism is classified as non-significant if it can be shown that the concrete enclosure is either not susceptible to the mechanism or affected by it to such a small degree that the intended function, namely providing a structural barrier to HLW or SNF, will be maintained during the remaining service life of the containment. A rapid age-related degradation mechanism is defined as potentially significant when, if allowed to continue without mitigating measures, it cannot be shown that the concrete would continue to maintain its structural capability during the design life of the structure (normally 50 or so years). Such degradation requires continuing mitigating measures. Potentially non-significant degradation mechanisms are those that are not expected to cause concern during the structure's design life but could fail in long-term analysis.

A third subsection has been added to discuss deterioration of refractory concrete. The deterioration mechanisms are the same, but this special concrete offers protective benefits. The section is provided since several of the concrete structures used to store HLW and SNF contain some refractory concrete to minimize the otherwise harmful effects of high temperature.

2.1 Potentially Significant Aging Degradation Mechanisms

This section contains a discussion of the potentially significant degradation mechanisms of concrete and reinforcing steel. The potentially non-significant mechanisms are discussed in Section 2.2. To the extent that available information permits, this section also contains quantitative interpretations of these mechanisms.

2.1.1 ELEVATED TEMPERATURE

When conventional (non-refractory) concrete is exposed to sufficiently elevated temperatures, it begins to dry (evaporation of the adsorbed and combined moisture present in the dried cement structure). The high temperature may increase thermal incompatibilities between paste and aggregate, and eventual deterioration of some possible constituents of the aggregate may occur from phase changes if the temperature becomes high enough and suitable aggregates were not used. Typically, such degradation is accompanied by a decrease in the compressive strength and in the stiffness (modulus of elasticity) of the concrete. Generally speaking, the threshold of degradation in the concrete is at a temperature range of 66°C to 95°C (150°F to 200°F). Because the high-level wastes and commercial SNF may reach a temperature in the range of 150°C to 180°C (302°F to 356°F), the exposure to elevated temperature could be a significant age-related degradation mechanism for the concrete enclosures. It is possible that creep of concrete at an elevated temperature under a sustained load could have an adverse effect on the concrete structure over a period of time. A detailed review of this significant aging degradation mechanism is provided in a BNL report [Ref. 2.2].

The compressive strength of concrete will be reduced when the concrete is exposed to a high temperature. A compilation of experimental data, obtained from a literature search, shows the loss of concrete strength (Figure 2-1) [Ref. 2.2]. The residual strength is expressed as percentage (%) of the 28-day strength. The upper- and lower-bound strength curves represent the full spread of the data base. The variations of the mean and 84% compressive strengths (based on standard log-normal distribution of the data) with rise in temperature are also shown. It is clear that the upper bound of the test data indicates almost no reduction in the concrete strength for elevated temperatures through almost 315°C (600°F). The lower bound data, however, indicate a reduced strength for temperatures above 38°C (100°F). For example, for specimens tested at 149°C (300°F), the lower-bound strength is about 60% of the initial compressive strength while the mean reduced strength is about 80% of its original value.

The modulus of elasticity, or stiffness, of concrete is a measure of its ability to withstand deformation. Figure 2-2 shows experimental data available in the literature indicating reduction in the modulus of elasticity, E_c, (expressed as % of the initial room temperature value) with increase in temperature [Ref. 2.2]. At 38°C (100°F), the upper-bound envelope indicates no reduction in the modulus while the lower-bound curve reveals a reduction of about 20%. At 149°C (300°F), the upper-bound curve indicates a modulus of 0.9 E_c while the lower-bound curve shows a modulus of 0.45 E_c. This indicates that in the temperature range of concern for these concrete applications, the reduction in the stiffness of concrete is more pronounced than that of the compressive strength. As shown in Figure 2-2, the reduction in modulus of elasticity at temperatures higher than 149°C (300°F) is significantly greater.

The above information on reduction of the compressive strength and modulus of elasticity is generic since it was extracted from a study of a vast database that includes experimental results of concrete specimens from a wide variety of sources, including tests performed on aged concrete from HLW tank farms (an underground HLW tank used to store liquid wastes). For example, in 1981, 3-inch diameter concrete core specimens were drilled from the wall of an empty single-shell tank [Ref. 2.3]. The tank was built in 1953 and was known to have leaked in 1965. It is also known that it held about 700,000 gallons of waste for about 8 years at temperatures which reached the range 127° to 138°C of (260° to 280°F). The specimens, which included samples extracted from different elevations of the wall

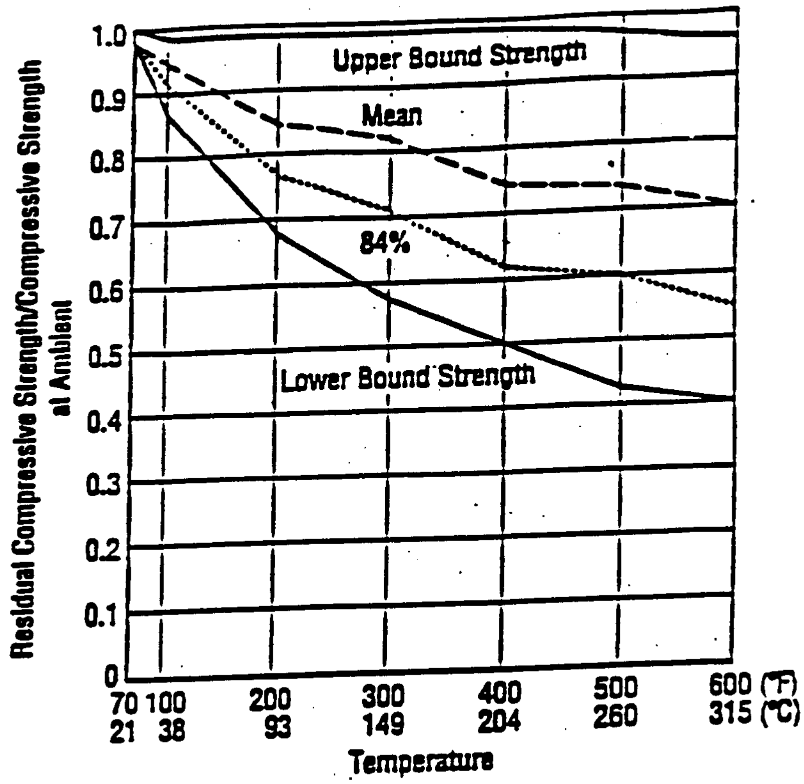

Figure 2-1. Compressive strength of concrete at elevated temperatures.

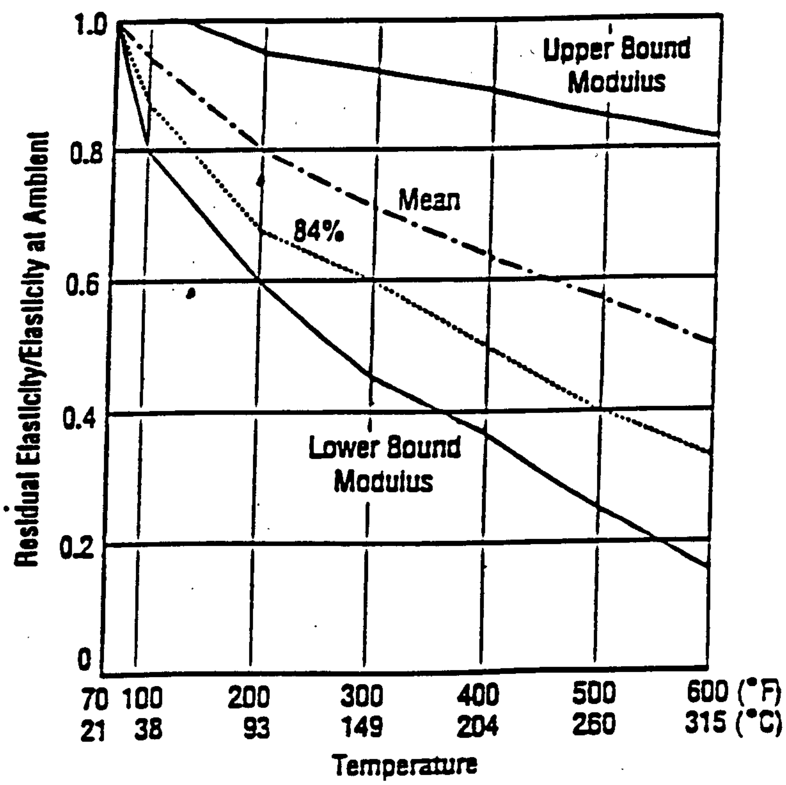

Figure 2-2. Modulus of elasticity of concrete at elevated temperatures.

excluding the lower portion near the foundation, were tested in the laboratory to determine the influence of elevated temperatures and aging on the strength properties of the concrete. The compressive strengths of all the specimens were found to exceed the 3,000-psi design strength [Ref. 2.3]. However, since the real initial strength data were not known, the results could not be used to determine whether there was any strength reduction.

If the bulk operating temperature of the concrete is maintained below the degradation level of 66°C (150°F), exposure of the concrete to elevated temperature is not a significant age-related degradation mechanism. The design codes allow a temperature rise up to 66°C (150°F) without any damaging effect on concrete [Ref. 2.4]. For those concrete structures suspected of achieving higher temperatures any time during the service life, the aging degradation due to elevated temperature could be a significant issue. The degradation in strength and modulus of elasticity are not recoverable when the temperature returns to lower operating temperatures. Additional information may be found in a BNL report [Ref. 2.2].

In underground concrete vaults, a thermal gradient is expected to exist between internal and external faces of the wall so that the entire concrete wall or floor may not be subjected to the same amount of thermal damage. Such site-specific conditions need to be considered for realistic estimates of concrete degradation. This is probably a less significant consideration for surface structures that transfer the heat to the air since the air has a lower heat transfer coefficient, thus the temperature on the outer surface of the concrete is expected to be higher than for the condition of transferring the same heat to the ground heat sink. Many of the concrete containers considered in the No-Action Alternative are designed for internal air cooling and thus transmission of heat through the concrete with its thermal gradient will not be the primary source of cooling for SNF or HLW. As long as this external air is circulating through the concrete to remove the heat, the concrete containers/shields should not exceed the design temperatures. For example, NUHOMS concrete storage casks are designed for short-term temperatures of 343°C (650°F) and long-term temperatures not exceeding 65°C (150°F).

If these air flow paths are plugged during the failure scenario, the external air cooling will no longer be effective and the concrete temperature will rise significantly if the SNF is still generating significant heat. In NUHOMS-07P Demonstration Project [Ref. 1.1], the calculated concrete temperature was estimated to be 75°C (168°F) with the expected cooling air flow, increasing to 160°C (321°F) when the lower air inlets were plugged, and further increasing to 232°C (450°F) when both the inlet and outlet air ports were plugged. A temperature rise in the concrete also influences the strength properties of the embedded reinforcing steel. Up to a temperature rise of about 371°C (700°F), experiments have shown that hot-rolled reinforcing steels exhibit a linear decrease in yield strength of about 15%. More pronounced reductions are observed at higher temperatures. In addition, as concrete and reinforcing steel have different coefficients of thermal expansions, the local bond strength may be influenced by a rise in temperature. Limited data under laboratory-controlled conditions have indicated that the loss in bond strength between the concrete and reinforcing steels in the temperature range of interest is in the range of 0 to 15% [Ref. 2.2].

2.1.2 FREEZING AND THAWING

Concrete exposed to extreme cold and situated at sites with significant rainfall or wet soils that freeze are potentially vulnerable to damage due to freezing and thawing. This leads to eventual degradation of the concrete. Water freezes within the capillary pores of concrete, creates hydraulic pressure which either increases the size of the cavities due to ice formation, or forces water into small voids in the surrounding areas created by entrained air bubbles. This results in cracking, scaling, and spalling. In extreme cases, the degradation could expose the reinforcing steel to accelerated corrosion, and the resulting expansion from the corrosion products deteriorates the concrete further and could reduce its strength and loosen the bond between concrete and the embedded steel. The primary parameters that affect the occurrence of such degradation in concrete include the air content of concrete and the number, size, and distribution of the pores within the aggregate of the concrete [Ref. 2.5]. The air content of the mixture needed to prevent such damage should meet the minimum requirement of Building Code ACI 318 [Ref. 2.6].

The following factors increase the resistance of concrete to degradation due to freezing and thawing:

- Adequate entrained air-void system in the cement paste (4% to 7%)
- Frost-resistant aggregate
- Low water/cement ratio and adequate placing and curing

Degradation due to freezing and thawing may be a significant issue for surface concrete storage casks stored on the surface when the heat load of the SNF has dissipated. For underground structures, where the concrete will not freeze repeatedly, the freeze-thaw failure degradation should not be significant.

The environment is measured in terms of "Weathering Index," which is defined as the product of the average number of freezing cycles times the average annual winter rainfall. ASTM C 33, "Standard Specification for Concrete Aggregates" [Ref. 2.7], groups the United States into "severe," "moderate," and "negligible" weathering regions. Freezing and thawing damage potential is "severe" where the index exceeds 500 day-inches (1,270 day-centimeters), "moderate" between 100 and 500 day-inches (254 and 1,270 centimeters-days), "negligible" when it is less than 100 day-inches (254 day-centimeter). If the concrete meets the air content and water-cement ratio requirements of ACI 318 [Ref. 2.4], then freeze-thaw damage should not be significant for design periods of 50 years for the "negligible" and "moderate" regions. Longer term evaluations in the Yucca Mountain EIS No-Action Scenario must consider this mechanism by considering the freeze-thaw cycles in the longer periods. For exposed concrete surfaces situated in "severe" weather regions, the degradation of affected surfaces of concrete could be significant and requires inspection and evaluation. This is a lesser concern for underground structures.

NUREG/CR-5542 [Ref. 2.8] describes other models for estimating freeze/thaw damage to concrete. That reference discusses several models used to determine freeze/thaw damage and they all seem to use comparable approaches but require different input data. The NRC suggested model is called the "Barrier Code" and requires the number of freeze/thaw codes as input. This information is not available from the 30-year history. Thus it was not used.

2.1.3 LEACHING OF CALCIUM HYDROXIDE

Water flowing through cracks or inadequately prepared construction joints in the concrete structures can dissolve the calcium-containing products in concrete. The most readily soluble material is calcium hydroxide (hydrated lime). When calcium hydroxide has been leached away, other cementatious constituents become exposed to chemical decomposition, which eventually could leave behind silica and alumina gels with little or no strength [Ref. 2.9]. Leaching over long periods increases the porosity and permeability of concrete, making it more susceptible to other forms of aggressive attacks and eventually reducing its strength and stiffness. Generally speaking, leaching also lowers the pH of concrete and allows corrosion of the reinforcing steel.

Concrete vaults that are exposed to groundwater may be susceptible to the same type of leaching of calcium hydroxide. In order to cause leaching, the water must be flowing, not just filling a crack or a void. For vaults situated in such an environment, the aging degradation mechanism is plausible and needs to be considered. Moreover, dense and well-cured concrete usually develops low permeability, minimizing the possibility of degradation caused by leaching of the calcium hydroxide.

Manifestation of damage by calcium hydroxide leaching is the appearance of white deposits (leachates) on the surface of concrete. Leaching of this material from the concrete increases the permeability of the concrete and could lower its pH, thereby making it more susceptible to attack by other damaging mechanisms (e.g., freezing and thawing and corrosion of the reinforcing steel). Quantifying the degradation is difficult. Inspection of the suspected surfaces should reveal the degree and extent of degradation.

2.2 Potentially Non-Significant Aging Mechanisms for Concrete

This section contains a discussion of the aging mechanisms the effects of which are non-significant for the concrete subjected to the present design standards and design lives. These mechanisms should not be of concern for short-term storage of HLW and SNF but may be significant in the long-term. A poor design or construction process may also lead to manifestation of any of these mechanisms during the life of the concrete. Such design and construction-related deficiencies are not addressed in the following assessment.

2.2.1 AGGRESSIVE CHEMICAL ATTACK

Because of the high alkalinity of concrete (pH > 12.5), strong acids cause degradation [Refs. 2.9, 2.10, and 2.11]. Sulfates in the soil and groundwater are potential sources of chemical attack on concrete. Chemical attack usually increases the porosity and permeability of concrete, reduces its alkaline nature, and subjects it to further deterioration, which can result in reduced compressive strength and stiffness. Sulfates typically attack concrete by reaction with the aluminate phase in the cement to produce internal expansion and cause degradation if the concrete was not made using sulfate-resisting cement. Sulfate attack is usually accompanied by expansive stress within the concrete, which can lead to spalling, cracking, and strength loss. Chlorides lower the pH of concrete and can cause corrosion.

The result of this degradation mechanism is an erosion of the cement in the concrete, which reduces the compressive strength and increases the porosity. The outward manifestation is a "pock marked" surface, which may ultimately lead to spalling. Quantifying the degradation is difficult; however, inspection should reveal the extent of the degradation.

For concrete below grade, the critical zone occurs along the exterior surface where the groundwater table fluctuates. The environment in contact with the concrete surface must have a pH level of less than 5.5 for this attack to occur. The minimum chloride concentration for potential corrosion of the reinforcing steel is approximately 500 parts per minute (ppm). A concentration of 1,500 ppm sulfate (water-soluble SO_4) is the minimum degradation threshold limit when Type II cement is used while a concentration of over 150 ppm may cause degradation when Type I cement is used in the concrete.

This form of degradation is normally severe if the concrete is exposed to strong acids such as those in chemical processing facilities. Since these conditions are not expected to exist in HLW and SNF storage, this mechanism is not considered to be a "significant mechanism." It is included as a non-significant mechanism potentially affected by site-specific conditions and long-term conditions to be evaluated in the No-Action scenario.

2.2.2 CORROSION OF REINFORCING STEEL

Concrete is a highly alkaline material (pH > 12.5) which provides an ideal environment to protect the embedded reinforcing steel rods from corrosion. However, when the pH of the environment in contact with the steel is reduced below the threshold level of 11.5, then corrosion of the embedded steel can occur [Refs. 2.12 and 2.13]. Concrete surfaces that are continuously exposed to aggressive environments are susceptible to embedded steel corrosion. The corrosive agents could have access to the steel through cracks in the concrete. The concrete considered in the No-Action scenario should not be exposed to an aggressive environment, but the same processes occur for benign environments over long periods of exposure. A reduction in the pH requires an ongoing intrusion of aggressive ions, most notably, chlorides in the presence of oxygen. The chloride ions cause a breakdown of the normal passive condition of the steel in the pore solution of portland cement and cause the corrosion. Calcium chloride accelerates the corrosion more than sodium chloride. Leaching of the alkaline products in the concrete through cracks or carbonation can also result in lower pH in concrete. In addition to the corrosive agents, the severity of corrosion is influenced by the quality of concrete (cement type, properties of aggregates, and moisture content), depth of concrete cover over steel, and the permeability of concrete. Generally speaking, concrete with low permeability contains less water and hence is more likely to have low electrical conductivity and better resistance to corrosion. Such concrete also provides a barrier to oxygen which is an essential element of the corrosion process.

Solid corrosion products of steel have a volume greater than that of the original metal. When corrosion occurs, this factor will subject the concrete to stress, eventually causing hairline cracking, followed by rust staining, spalling, and more severe cracking. Such development may expose more of the reinforcing steel to the corrosive environment and the concrete to further degradation. The degradation in concrete is usually manifested by a reduction in its strength, stiffness, and other physical properties, and a loss of bond between concrete and embedded steel. A reduction in the cross sectional area of the steel can occur which ultimately could impair the structural integrity of the concrete enclosure of the tanks.

Corrosion of the reinforcing steel in concrete is an electrochemical reaction between the reinforcing steel and its surrounding environment. It occurs whenever the oxide film, formed during cement hydration and maintained by the alkalinity of the concrete, is broken by the intrusion of corrosive ions (mainly chlorides) from the environment. Laboratory simulation indicates that the threshold for Cl^-/OH^- in the concrete pores necessary to cause corrosion is approximately 0.3 [Ref. 2.14]. This is equivalent to a pore water chloride level of about 9,000 ppm. For surface concrete structures, significant corrosion is thought to occur when the chloride ion concentration reaches 0.35 to 1.0% by mass based on cement content of the concrete. Slower corrosion will occur for the environment expected in the No-Action scenario. The quality of concrete and its permeability play a major role in its resistance to intrusion of chloride ions and the resulting corrosion.

2.2.3 REACTION OF AGGREGATES WITH ALKALINES

Certain concrete aggregates can react chemically with alkaline introduced in the cement or from the environment [Ref. 2.15]. Two types of reactions, alkali-silica and alkali-carbonate, have been identified. Moisture must be available for the chemical reactions to occur. Thus, concrete that is either consistently wet or that experiences wet and dry periods is susceptible to such deterioration in the presence of potentially reactive aggregates. The chemical reactions can cause expansion and irregular map cracking of the concrete. Most reactive aggregates have been identified and, when they are used, appropriate precautions can be taken: low-alkali cement is required and additional protection can be obtained from the use of ground slag or pozzolan, such as flyash or silica fume. Good design specifications should minimize this mechanism.

2.2.4 CREEP AND SHRINKAGE

Creep is defined as an increase in inelastic strain with time under a sustained stress. The stress results from dead load, live load, and the effects of elevated temperature on the concrete. The influence of elevated temperature on creep is discussed in [Ref. 2.2]. Creep strain, which varies exponentially with time, can cause cracking at the aggregate cement-paste interface. Except for the creep strain induced by elevated temperatures as mentioned in Section 2.1.1, creep-induced concrete cracks are usually small and do not result in concrete deterioration, nor do they reduce the compressive strength by significant amounts. Guidance for predicting creep in structures is available in ACI 209 [Ref. 2.16].

Shrinkage of concrete occurs as a result of water leaving the concrete. As water leaves the concrete, tensile stresses remain in the concrete. When the strains produced by these stresses exceed the tensile strain capacity of concrete, a shrinkage crack is formed. Excessive shrinkage may cause cracking of concrete surfaces. Most of the shrinkage (98%) typically occurs during the first few (e.g., five) years of service. The significance of a shrinkage crack as a potential contributor to degradation depends primarily on its size and environmental exposure conditions. A crack can allow aggressive agents access to the reinforcing steel, promoting the possibility of corrosion.

If the concrete is designed and constructed according to standard codes, the shrinkage degradation should not be significant.

2.2.5 ABRASION AND CAVITATION

Abrasion and cavitation are age-related degradation mechanisms for concrete exterior surfaces of the concrete that are continuously exposed to flowing water moving at high velocity or carrying suspended solids. As the water moves over concrete surfaces, it has the ability to transport materials that can abrade the concrete. It also can create negative pressure at the water/air-to-concrete interface that can result in removal of concrete materials as the vacuum collapses (cavitation). Cavitation can occur at velocities as low as 25 feet per second at abrupt changes in slope or curvature [Ref. 2.17]. If significant amounts of concrete are removed by this mechanism, visual inspection will reveal the degradation by pitting or aggregate exposure due to loss of cement paste. This is very unlikely to be significant to the concrete structures. These modes of degradation are significant to bridges over water, etc., but are not expected to be significant to the No-Action applications.

2.2.6 IRRADIATION

The degradation of concrete exposed to neutron and/or gamma radiation is manifested in many ways. Fast and slow neutrons usually cause aggregate growth, decomposition of water, and warming of concrete. Gamma radiation affects the cement paste portion of the concrete, producing heat and causing water migration. The degradation due to nuclear heating and water loss is more serious than degradation associated with direct radiation damage [Ref. 2.18]. This is because nuclear heating causes the free water within the concrete to evaporate, and both the neutron shielding and structural characteristics of the concrete become impaired. As a consequence, the concrete could experience a decrease in its strength (compressive, tensile, and bonding strengths) and stiffness (modulus of elasticity) from shrinkage and cracking if the thermal gradient is excessive.

According to the American National Standard ANSI/ANS-6.4-1985 [Ref. 2.19], nuclear heating can be neglected if the incident energy fluxes are less than 1,010 MeV/cm^2-sec. Existing information [Ref. 2.17] indicates that the strength properties of concrete (compressive strength and modules of elasticity) are degraded if the concrete is exposed to greater than 10^{19} n/cm^2 or to an integrated dose of gamma radiation exceeding 10^{10} rads. In the conditions assumed, the energy flux is negligible and irradiation is a non-significant aging degradation mechanism.

2.3 Degradation of Refractory Concrete

Refractory concrete consists of graded, refractory aggregates bound by a suitable cementing medium. It is suitable for use elevated temperatures up to about 1,800°C (3,272°F) when calcium-aluminate cement is used with fused-alumina aggregate [Ref. 2.20]. The cementing agent commonly used is high-alumina cement, which is a hydraulic cement unlike Portland cement [Ref. 2.21]. However, when Portland cement is used as the binder, refractory concrete loses some of its strength and performs poorly when thermally cycled to temperatures above 430°C (806°F), especially in the presence of moisture. In several of the storage facilities, refractory concrete is used to protect the bulk of the concrete from thermal effects of SNF or HLW. This special concrete is supported by conventional reinforced concrete.

The properties of refractory concrete depend on both time and temperature. Possible age-related degradation mechanisms are discussed in the following two subsections.

2.3.1 ELEVATED TEMPERATURE

Initial heating of refractory concrete causes physical and chemical changes mainly due to removal of water. The compressive strength is reduced after exposure to about 540°C (1,004°F) but further increase in the temperature does not influence the strength [Ref. 2.15]. The effect of elevated temperature on the modulus of elasticity is relatively insignificant. Exposure to hot moist environment greatly reduces the compressive strength unless a rich dense mixture has been used [Ref. 2.22].

2.3.2 EFFECTS OF CHEMICALS

Refractory concrete can be corroded by acid that condenses on the cold face of the steel liner if the cold face temperature is below the dew point [Ref. 2.23]. Concrete made using high-alumina cement can suffer major losses in strength when exposed to moisture at relatively low temperatures due to conversion of the unstable low-density to the stable high-density calcium-aluminate hydrate. Formation of high density alkali-alumina silicates can cause disintegration of the refractory concrete [Ref. 2.21].

2.4 Section 2 References

2.1 Bandyopadhyay, K. K., S. Bush, M. Kassir, B. Mather, P. Shewmon, M. Streicher, B. Thompson. D. van Rooyen, and J. Weeks, 1997, *Guidelines for Development of Structural Integrity Programs for DOE High-Level Waste Storage Tanks*, Brookhaven National Laboratory Report BNL-52527, January.

2.2 Kassir, M. K., K. K. Bandyopadhyay, and M. Reich, 1996, *Thermal Degradation of Concrete in the Temperature Range from Ambient to 315°C (600°F)*, BNL Report, No. 52384, Revised October.

2.3 Defigh-Price, D., 1994, *Strength and Elastic Properties of Concrete Exposed to Long-Term Moderate Temperatures and High Radiation Field*, American Concrete Institute Fall Convention, Rockwell International Report RHO-RE-SA-55R.

2.4 ACI (American Concrete Institute), 1963 and later editions, *Building Code Requirements for Reinforced Concrete*, ACI Standard 318, ACI Committee 318, Detroit, Michigan.

2.5 Mather, B., 1990, *How to Make Concrete that Will Be Immuned to the Effects of Freezing and Thawing*, in Paul Klieger symposium on Performance of Concrete, David Whiting (editor), American Concrete Institute, SP-122, pp. 1-18, Detroit, Michigan.

2.6 ACI (American Concrete Institute), 1994, *Building Code Requirements for Reinforced Concrete*, ACI 318, (Revised 1992), ACI Manual of Concrete Practices, Part III, Detroit, Michigan.

2.7 ASTM (American Society for Testing and Materials), *Standard Specification for Concrete Aggregates*".ASTM C 33, Philadelphia, Pennsylvania, Annual.

2.8 Watson, J. C., Plansky, L. E., and Smith, R. W., "Models for Estimation of Service Life of Concrete Barriers in Low-Level Radioactive Waste Disposal," NUREG/CR-5542, U.S. Nuclear Regulatory Commission, prepared by EG&G Idaho (Report EGG-2597).

2.9 Troxell, G. E., H. E. Davis, and J. W. Kelly, 1968, "Composition and Properties of Concrete," Second Edition, McGraw-Hill.

2.10 Mehta, P. K., 1986, "Properties and Materials," Concrete-Structure, Prentice-Hall, Inc., Englewood Cliffs, New Jersey.

2.11 Mindess, S. and J. F., Young, 1981, *Concrete*, Prentice Hall, Inc. Englewood. New Jersey.

2.12 Brewer, K. N., 1993, *Effects of Rebar and Concrete Construction Joints on the Migration of 4M HNO3 in Concrete Test Cylinders*, Idaho National Engineering Laboratory, WINCO-1125, June.

2.13 ACI (American Concrete Institute), 1993, *Corrosion of Metals in Concrete*, ACI 222R-89, American Concrete Institute Manual of Concrete Practice, Part 1, Detroit, Michigan.

2.14 Hsu, T. C., et al., 1993, *Savannah River Site Waste Tank Corrosion Program (U)*, WSRC-TR-93-373, Draft, September.

2.15 ACI (American Concrete Institute), 1993, *Guide to Durable Concrete*, Committee 201, Chapter 5, Report 201.2R-92, American Concrete Institute Manual of Concrete Practice, Part 1, Detroit, Michigan.

2.16 ACI (American Concrete Institute), 1993, *Prediction of Creep, Shrinkage, and Temperature Effects in Concrete Structures*, ACI 209-92, American Concrete Institute Manual of Concrete Practice, Part 1, Detroit, Michigan.

2.17 ACI (American Concrete Institute), 1993, *Erosion of Concrete in Hydraulic Structures*, ACI 210R-87, American Concrete Institute Manual of Concrete Practice, Part 1, Detroit, Michigan.

2.18 Hilsdorf, H. K., J. Kroop, and H. J. Koch, 1978, *The Effects of Nuclear Radiation on the Mechanical Properties of Concrete*, Douglas McHenry International Symposium on Concrete and Concrete Structures, American Concrete, Publication SP 55-10, pp 223-251.

2.19 ANC (American Nuclear Society), 1985, *Guidelines on the Nuclear Analysis and Design of Concrete Radiation Shielding for Nuclear Power - Plants*, American National Standards, ANSI/ANS-6.4-1985, LaGrange Park, Illinois.

2.20 ACI (American Concrete Institute), 1979, *Refractory Concrete*, ACI Committee 547, ACI 547 R-79, American Concrete Institute, Detroit, Michigan.

2.21 Robson, T. D., 1962, *High-Alumina Cements and Concrete*, John Wiley and Sons, New York.

2.22 Naus, D. J., 1988, *A Review of the Effects of Elevated Temperature on Concrete Materials and Components with Particular Reference to the Modular High Temperature Gas-Cooled Reactor (MHTGR)*, ORNL/NRC/LTR-88/2, LTR CTP-8801, Concrete Technology Program, Oak Ridge National Laboratory, Oak Ridge, Tennessee, March.

2.23 Gitzen, W. H., et al., 1964, *Carbon Monoxide Disintegration of Calcium Aluminate Cements in Refractory Castables*, Amer. Cer. Soc. Bull. 43(7).

CHAPTER 3. PREVIOUS FAILURE ANALYSES SIGNIFICANT TO THE YM EIS

A number of performance analyses have been prepared for waste facilities contained in a concrete housing like that being assumed for the YM EIS No-Action Scenario. Sections 3.1 and 3.2 summarize pertinent parts of several of these performance assessments as they relate to concrete facilities housing for HLW or SNF at the generator sites. Appendices A and B provide more detailed information on these assessments.

3.1 Surface Storage Summary

A single performance assessment was reviewed for **surface storage**. It was previously discussed [Ref. 1.2] in the NRC SER for NUHOMS-24P concept. This report evaluated the high temperature effects on the concrete storage casks and concluded that:

- "Given the maximum concrete design temperature of the NUHOMS-24P HSMs (i.e., less than 150°F for the 70°F lifetime normal ambient case and less than 200°F for the maximum normal summer ambient case of 100°F) the concrete integrity is unaffected...."

- "For the worst case accident condition with the HSM vents assumed to be blocked during an extreme ambient temperature of 125°F for which the maximum HSM and the concrete temperature are less than 350°F, except at local areas near the center of the roof and floor slabs. At these locations the maximum concrete temperatures are 365°F and 395°F."

The functional intent of this SER was to evaluate the NUHOMS HSM and determine its safety for use in storing PWR SNF for up to its 50-year licensed life time. The NRC found that the NUHOMS-24P HSM was a safe storage package for this time period. Appendix A provides more of the details of the performance assessment of the concrete HSM.

3.2 Underground Storage Summary

Four performance assessments were reviewed to see how pertinent they were to establishing input for the No-Action analysis of **underground concrete facilities**. Three of the four performance assessments were for low-level waste RCRA facilities. The fourth was an industrial wastewater closure. All required an extensive water protection barrier to cover (very similar or equivalent to a RCRA cap) the concrete structure to minimize vadose zone water flow and permeation of the concrete.

Only one of the four concrete structures, the E-Area vaults at SRS, had an unsupported concrete roof as exists for HLW underground structures [Ref. 3.1]. The vaults are typically 58 meters long, 15 meters wide, and 8.8 meters high. The normal grade is near the top of the vault, which will receive a RCRA-type cover. Three types of structures were analyzed in this performance analysis: Intermediate Level Tritium Vaults (ILT), Intermediate Level Non-Tritium Vaults (ILNT), and Low Activity Waste Vaults (LAW). Each have slightly different designs and physical dimensions but are evaluated in the same manner.

The performance assessment considered a combination of physical, chemical, and mechanical processes that will cause vault degradation. Physical and mechanical degradation processes that cause cracking of the concrete could increase permeability.

Sulfate attack, carbonation, calcium hydroxide leaching and reinforcing bar corrosion could disrupt the integrity of the concrete structure. A special study conducted by an independent engineering firm evaluated degradation mechanisms and their effect on integrity of the vault system. The results of this study predicted the time required for cracking of the vault and collapse of the roof structures and predicts the following time to failure:

Vault design	Estimated time to onset of failure (years)		
	Roof cracks	Wall cracks	Roof collapse
ILNT	570	800	1,045
ILT	790	1,080	1,300
LAW	1,420	2,235	3,100

Another performance assessment for SRS Z-Area Saltstone Disposal Facility [Ref. 3.2] reaches similar values. In this reference, the concrete vault is filled with saltstone (a LLW residue solidified with grout) and clean grout is used to completely fill the vault. This action eliminates the roof collapse scenario. The performance assessment evaluates sulfate attack, carbonation, calcium hydroxide leaching, and reinforcing bar corrosion. The analysis concludes that sulfate attack for the relatively pure water percolating through the vadose zone will result in no perceptible sulfate corrosion in 10,000 years. Sulfate corrosion in the saltstone pore fluid has been measured at about 25,000 mg/L. Sulfate leached from the waste form will first contact the inner wall of the vault and cause corrosion on the inner surface. The performance analysis made no attempt to evaluate when failure due to this mechanism would occur because "the task of predicting concrete failure for this case is very complex." The performance assessment evaluated carbonation and predicted it would affect only 15 cm of the wall and roof in the 10,000 year assessment. (Concrete wall and roof thickness are 460 and 760 cm, respectively.) The performance assessment estimated that leaching (of calcium hydroxide) would require in excess of 5,000 years before the water permeation rate would significantly increase. The more limiting condition was corrosion of the reinforcing bar, which would result in wall-to-roof movement and increases permeation. This failure time was estimated to begin at 500 years and become significant at 2,000 years.

The industrial waste closure plan [Ref. 3.3] for SRS HLW tank closure presented failure information for the outer concrete enclosure for three assumed scenarios. Each of these evaluated closure of the waste tanks after they had been emptied, cleaned, and filled with either sand or engineered grout. These tanks have soil covers of about 10 feet for shielding. The three scenarios evaluated were grout fill and no RCRA type cap, grout filled and a RCRA type cap, and sand filled and no RCRA type cap. The assumed failure times for the concrete case were estimated to be 1,400, 2,000, and 1,500 years, respectively. In that closure analysis, increased permeability was assumed to occur after 1,000, 1,500, and 500 years, respectively, to add additional conservatism.

The Hanford interim performance analysis for Low-Level Tank Wastes [Ref. 3.4] contains no concrete enclosure failure analysis but makes the conservative analysis that all concrete structures are fully degraded after 500 years. They draw this conclusion because of the NRC's draft technical position [Ref. 3.5] recommending that no credit be taken for engineered physical components after at most 500 years.

This draft NRC technical position is being considered for performance assessments of low-level waste disposal facilities because it describes a conceptual system that considers infiltration, engineered barrier performance, waste form integrity and leachability, and transport pathways. Their system develops a complete view of how the system might perform, conducts consequence modeling to determine how uncertainty associated with an element affect the conclusions, and performs sensitive analysis to ensure that controlling variable(s) are well known and the disposal site has been appropriately analyzed. The NRC Waste Management technical position on performance of engineered barriers (as is being described in this paper) is that these barriers should be assumed to have physically degraded after 500 years, unless specific analysis can show longer life is appropriate based on "suitable information and justification and evaluated on a case-by-case basis."

The Branch's position is that after 500 years the engineering barriers can be assumed to continue to function but not at the same level as was designed: the function would be established based upon the properties of its constituent materials. This position recognizes that it is unreasonable to assume that any engineering barriers can be designed to function long enough to influence eventual release of long-lived radionuclides, such as carbon-14 (half-life: 5,700 years), technetium-99 (half-life: 214,000 years), and iodine-129 (half-life: 15,800,000 years), if they are present. This leads the Commission to propose a three-step approach: (1) service life of the engineered barrier, (2) time of decreasing function of the engineering barrier during its degradation, and (3) time when complete degradation has occurred. Complete degradation of the concrete barrier assumes return to the constituent sand and gravel. It is, however, reasonable to assume chemical buffering during phases two and three.

The Commission's paper provides some estimates of hydraulic conductivities for undegraded concrete structures to range between 1×10^{-11} to 1×10^{-9} centimeters/second. The paper doesn't provide judgments for phases 2 and 3 but indicates that engineering judgment must be applied in their development. They recommend for preliminary modeling that a step function be used, with the step occurring at the beginning of the time period. They further state for later iterations, it is permissible to model the failure as a continuous function in an attempt to reflect reality.

3.3 Section 3 References

3.1 Martin Marietta Energy Systems, Inc., EG&G Idaho, Inc., and Westinghouse Savannah River Company, 1994, *Radiological Performance Assessment for the E-Area Vaults Disposal Facility*, Report WSRC-RP-94-218, April 15.

3.2 Martin Marietta Energy Systems, Inc., EG&G Idaho, Inc., Westinghouse Hanford Company, and Westinghouse Savannah River Company, 1992, *Radiological Performance Assessment for Z-Area Saltstone Disposal Facility*, WSRC-RP-92-1360, December 18.

3.3 SRS (Savannah River Site), 1996, *Industrial Wastewater Closure Plan for F- and H-Area High Level Waste Tank Systems - Construction Permit Numbers 14,338, 14,520, and 17,424-IW*, June 1.

3.4 WHC (Westinghouse Hanford Company), 1996, *Hanford Low-Level Tank Waste Interim Performance Assessment*, WHC-EP-0884, Revision 0, September.

3.5 NRC (U.S. Nuclear Regulatory Commission), 1994, Branch Technical Position on Performance Assessment for Low-Level Disposal Facilities, Draft, January.

CHAPTER 4. PROPOSED FAILURE SEQUENCE FOR YM EIS NO-ACTION ANALYSIS

The approach proposed in this section is divided into two parts: (1) surface structures and (2) underground structures. These generic failure analyses are discussed in Section 4.1 for surface storage, Section 4.2 for underground structures in humid-mesic environments, and Section 4.3 for underground structures in arid-xeric environments.

The analytical approach proposed for the YM EIS No-Action alternative is to assume a four-step analytical approach similar to the NRC [Ref. 3.6] approach added to the institutional control period. Basic steps for surface structures are: (1) institutional control period; (2) service life of the engineered barrier, (3) period of onset of failure, (4) period of significantly decreasing function of the engineering barrier, and (5) time when complete degradation has occurred. The NRC paper provides estimates of facility leak rates (called hydraulic conductivities) for underground concrete structures (step 1) to range between 1×10^{-11} to 1×10^{-9} centimeters/second. Complete degradation of the concrete barrier assumes return to the constituent sand and gravel with hydraulic conductivities of 1×10^{-3} to 1×10^{-1} [Ref. 4.1].

The proposed approach for underground structures seems to be better described by a six-step process. The steps proposed combine facility degradation and characteristics of the SNF or HLW contained (i.e., heat generation, etc.)

4.1 Surface Structures

The conclusions for surface facility damage are shown on Table 4-1. Figure 4-1 is intended to show the type and extent of damage to surface storage facilities expected with respect to storage time. This figure doesn't include damage to dry storage canisters or to the SNF. The analysis contained in the remainder of this section leads to the conclusion that the major failure mechanism for surface concrete structures results from freeze/thaw and must use site-specific parameters during the actual analysis. The table also provides the assumed failure schedules for each phase for the three example locations.

Table 4-1. Proposed schedule for surface facilities using assumed conductivities and schedules.

Analytical phase	Conductivity (cm/sec)	Schedule of failure for Augusta, GA (years)	Cleveland, OH (years)	Saint Cloud, MN (years)
Institutional control period	1×10^{-10}	0 to 100	0 to 100	0 to 100
Full protective barrier	1×10^{-10}	100 to 118	100 to 109	100 to 109
Onset of failure of protective barrier	1×10^{-7}	119 to 260	110 to 179	110 to 181
Decreasing protectiveness of barrier	1×10^{-2}	261 to 1,000	180 to 1,000	182 to 1,000
Full barrier failure	1×10^{-2}	After 1,000	After 1,000	After 1,000

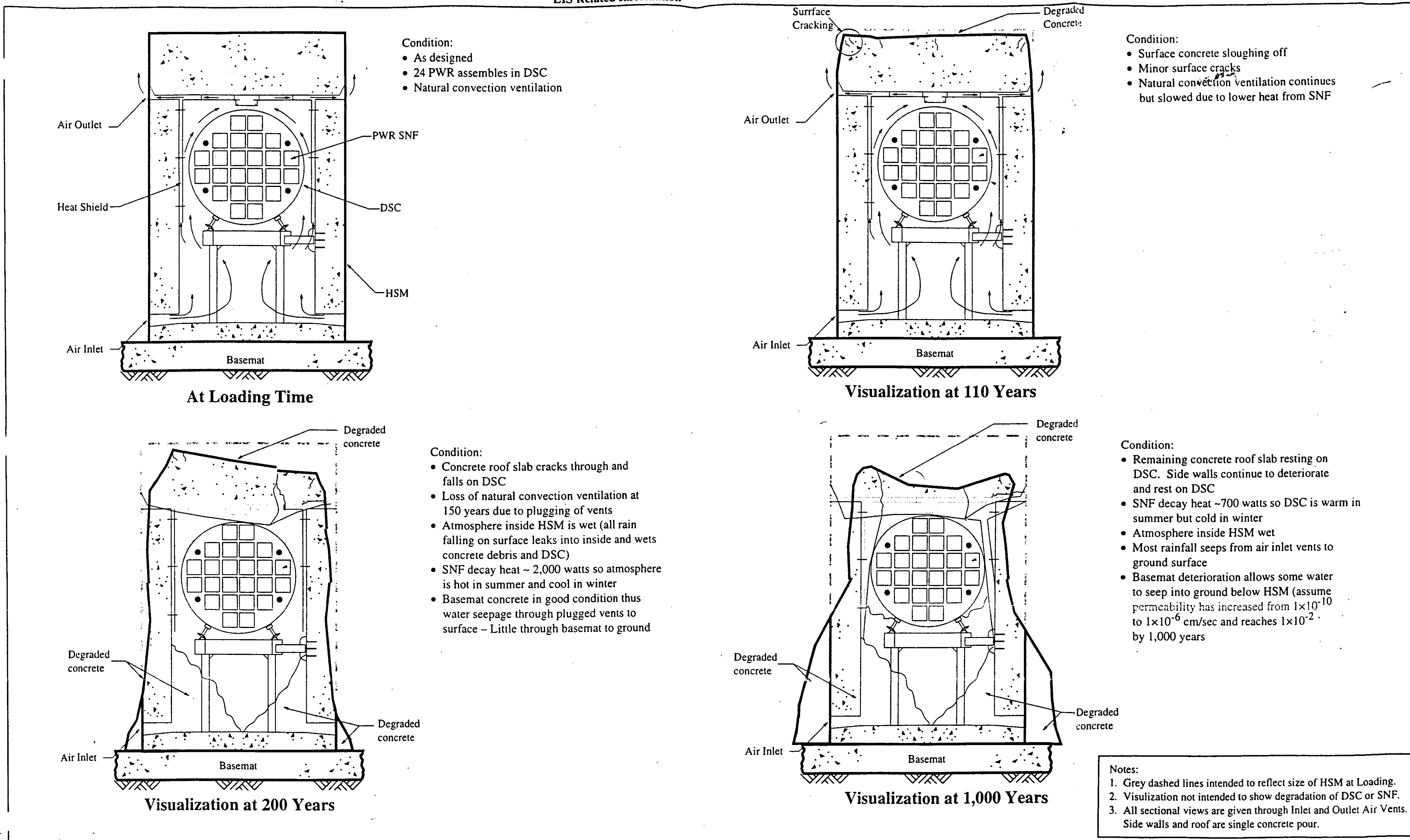

Figure 4-1. Graphical representation of failure of NUHOMS horizontal storage module (assumed location Cleveland, OH).

4.1.1 HIGH TEMPERATURE EFFECTS

The concrete NUHOMS-24P HSM is designed and constructed to withstand normal and off-normal conditions with a design life of 50 years. To establish the necessary structural resistance, the design considers the expected thermal load for storage of 24 PWR fuel (contained in a stainless steel canister) as shown on Figure 1-3. The HSM design considers the thermal effects of normal storage with maximum concrete temperatures of 215°F on the inside roof, 194°F inside base slab temperature, and 187°F on the outside roof for an assumed outside air temperatures of 125°F [Refs. 1.1 and 1.2]. The design also considers a short-term temperature excursion from HSM with plugged vents. The analysis assumes that the plugged vents are discovered and air flow corrected within 2 days. Should this excursion occur during an assumed 125°F ambient period during the summer, the temperature of the concrete would reach 395°F. The SER indicates the stresses in the concrete for these conditions will be a maximum of 81% of ultimate stress for the HSM, so no thermal damage is expected. Since the NUHOMS analysis did not calculate thermal equilibrium for the plugged vent scenario, it is reasonable that the temperature will exceed the listed values and that the temperatures might increase an additional 20%.

For the YM EIS No-Action alternative, it is reasonable to assume that during the 100-year period with institutional control, the HSM is under constant observation and the HSM will continue to provide the necessary protection for the SNF. Since the HSM is licensed for 50-year life, it will probably be necessary for the owner to extend the life of the HSM or change them out during the YM 100-year institutional control period. If an HSM is loaded with PWR SNF and at the design limit of 0.66 kW/PWR fuel assembly, the total HSM heat load will be 15.8 kW. If this loading time is assumed at the beginning of the 100-year institutional control, the thermal load of the HSM will be 4 kW at its end (see Figure 4-2). It is further reasonable to assume that with no surveillance, vent pluggage will occur. The time of pluggage is uncertain and is assumed to occur 50 years after loss of institutional control. Given the expected decay of the SNF over this 150-year period, HSM heat generation would have continued to decrease to 3 kW. At this thermal load, the HSM concrete temperature would reach a maximum floor temperature of ~200°F and a wall temperature of 180°F. These temperatures are essentially the same as described in the NRC SER for unplugged storage at 15.8 kW/HSM. At these temperatures, the water in the capillary pores of the concrete would be lost but the adsorbed waters in the concrete would be unaffected. This analysis concludes that this temperature range will cause no damage to shorten the concrete life.

4.1.2 FREEZE/THAW ANALYSIS

The mechanism of concrete freeze/thaw is dependent upon the location of the surface storage and the weather to which the HSM is exposed. Freeze/thaw damage results in concrete sloughing, cracking and increased permeability. When reinforcing rods are exposed, they begin to corrode much faster and lower the structural strength of the concrete. As indicated in Section 2, the weathering index is measured by the average number of freezing cycles times the average annual winter rainfall. Reference 2.7 provides some guidance that will be used to estimate this weathering. It states that concrete will not significantly weather in 50 years until the weathering index exceeds 500 day-inches. At values above that level, special protection has to be provided for the concrete. Table 4-2 shows this weathering for three representative cities located near nuclear power reactors. Since the YM EIS No-Action analysis considers 10,000 years, we should assume damage begins at an integrated weathering index of 25,000 day-inches. Since the "Local Climatological Data" does not distinguish between freezing while wet, using this data probably overstates freeze/thaw damage. For this analysis, we assume initiation of damage at 25,000 day-inches. For NUHOMS-type concrete structures, this can be thought of as concrete failure to a depth of the outer reinforcing rods (or 3 inches out of the 3-foot thickness of the concrete).

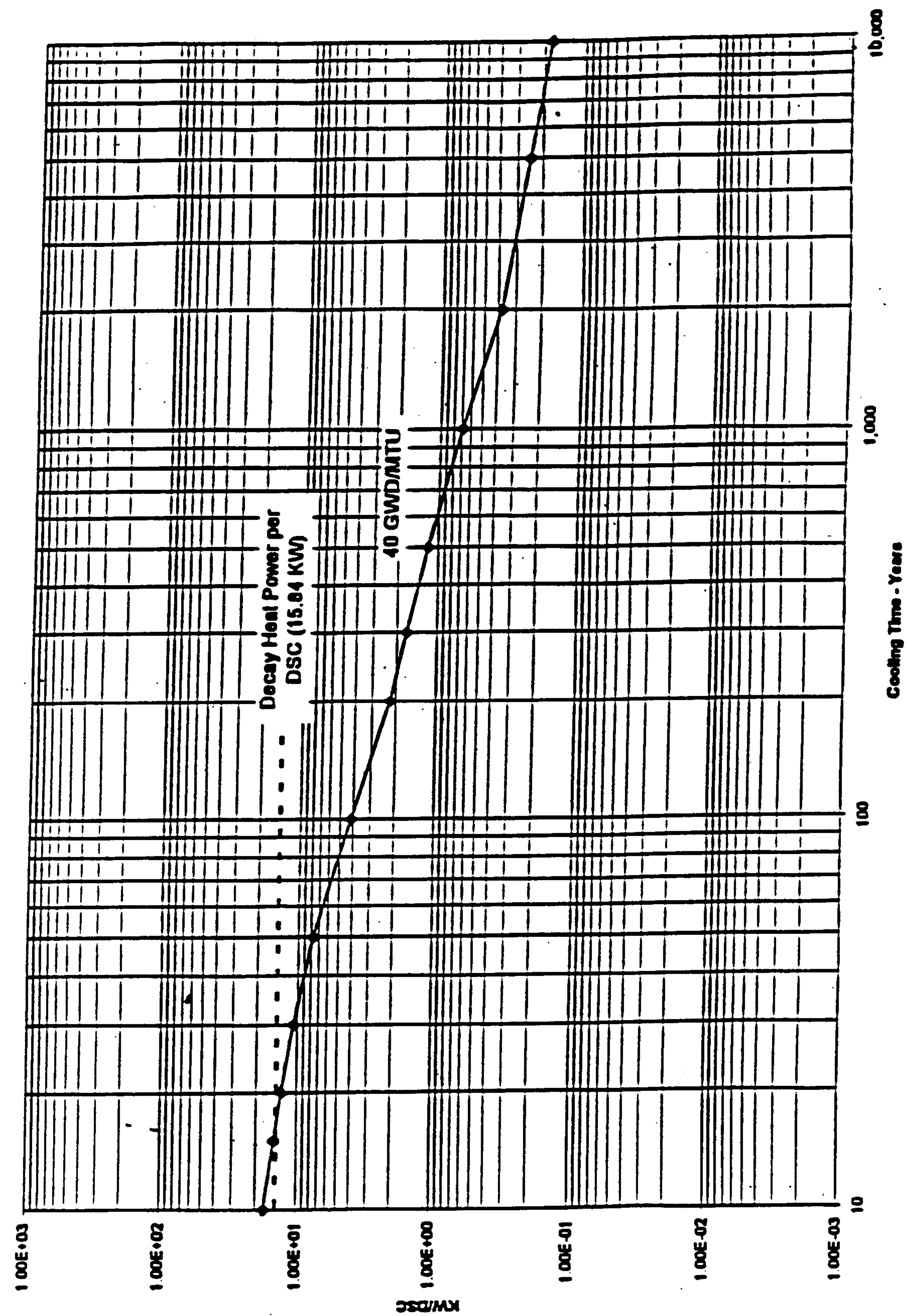

Figure 4-2. Thermal output of NUHOMS-24P DSC.

Table 4-2. Example information for concrete freeze/thaw weathering.

	Augusta, GA	Cleveland, OH	Saint Cloud, MN
Winter precipitation[a] (inches precipitation) precipitation during months with temperature falling below freezing.	25	22.6	15.8
Freezing (days/year)	56.2	126	177
Months with freezing	7	8	9
Weathering index (day-inches/year)	1,410	2,830	2,790
Onset of damage reached (years)	17.8	8.8	9.0
Roof collapse (years)	160	79	81

a. Number of freezes and precipitation use 30- to 40-year meteorological history [Ref. 4.2].

Since the as-built concrete structure has no significant exterior load and is a fairly thick concrete shield with no long overhangs that require significant structural support, it is judged that failure would not occur until the surface freeze/thaw damage proceeded half way through the thickness of concrete. This postulated failure is assumed to result in a collapse of the top of the concrete HSM, and thus the HSM will provide little further water infiltration protection. To determine the time for the freeze/thaw damage to proceed to 18 inches depth in the concrete, several assumptions were made. These assumptions include:

- The average freeze/thaw damage rate for onset damage was determined (Table 4-2)
- Freeze/thaw damage causing collapse of the roof should take at least 6 times that assumed for onset of damage (18 inches vs 3 inches)
- The average rate of freeze/thaw damage slows as the damage progresses into the concrete because of the protection provided by the surface concrete debris
- The slowing in the average freeze/thaw damage is assumed to add 50 percent to time for freeze/thaw damage to proceed to the half thickness of concrete. This is equivalent to adding a factor of nine to the time for initiation of failure.

An evaluation was made to see if these conclusions are affected by the self heat from the SNF in these surface storage facilities. Based upon information given in References 1.1 and 1.2, the outside top of the HSM, the coldest surface of the HSM, would be 11 degrees warmer that the air temperatures. This would offer marginal freeze/thaw protection at that time. This protective effect would decrease as the thermal output decreased due to decay of radionuclides in the SNF. The conclusions is that this self-protection is short lived and within the error assumed using average 30- to 40-year meteorological data.

4.1.3 OTHER DEGRADATION ANALYSIS

As described in Section 2, there are other mechanisms causing concrete degradation. These include sulfate and magnesium attack, calcium leaching carbonation, and chloride penetration. Each of these are ongoing at a much slower rate than for the freeze/thaw mechanism for most of the potential storage sites in the United States. For the three cities defined in Table 4-2, freeze/thaw degradation accounts for ~99.5% of the damage. There are reactor sites that have no freezing weather (South Florida, South Texas, and Southern California) where these other mechanisms become the predominate failure mechanisms. These degradation mechanisms are discussed in Section 2 and Appendix B of this report and are quantified in a report titled "National Weather Conditions Affecting Long-Term Degradation of Commercial Spent Nuclear Fuel and DOE Spent Nuclear Fuel and High-Level Waste," [Ref. 4.3].

Analyses of underground concrete facilities have shown that they are very slow. Reference 1.4 determined that it would require more than 1,000 years to leach the calcium from the E-Area Vaults at SRS to a depth of 0.05 centimeter. This analysis is described in Appendix B of this paper. If one adjusts this value to reflect surface facilities and the calcium content of the rainfall, the calcium leaching is reduced by about 30%. The more corrosive "acid rain" contains significant quantities of sulfate, magnesium, and chloride which influences this degradation. It is expected that chloride penetration may be the next most severe degradation for surface facilities.

4.2 Underground Structures in Humid-Mesic Environment

This section describes the judgment on failure of the GWSB and probably other underground structures with similar designs and thermal characteristics. This facility is assumed to be located in a humid-mesic environment where precipitation essentially equals or exceeds the evaporative capacity. SRS environment is assumed with average precipitation of 48 inches which is fairly evenly spread throughout the year [Ref. 4.4]. The evaporative capacity [Ref. 4.5] of this region is essentially the same as the precipitation, thus the region is normally humid. Of the 48 inches of precipitation, about 30% infiltrates into the surrounding soils [Ref. 4.6] and through the vadose zone reaching the water table that recharges the aquifer.

Figure 4-3 presents a plan view of the GWSB and Figure 4-4 provides two elevation views.

Location of the two elevation views is shown on Figure 4-3 [Refs. 1.3 and 4.7]. The glass storage vault is located below grade and is constructed of reinforced concrete designed to provide protection of the waste and protect workers from the radiation of the waste. The vault is primarily a Category I structure and weather protection is provided by a Category III building. This latter building has been designed to standard requirements with a design life of 50 years.

As indicated in Section 1.2, this GWSB is designed to store 2,286 canisters made of stainless steel containing borosilicate glass that has incorporated the HLW. These canisters are being stored in the GWSB until they can be shipped to the geologic repository. The building ventilation is designed to remove up to 750 watts decay heat from each canister of this HLW. This cooling is provided by operating supply fans, and the discharged heat is filtered before leaving the building. The design of the building will remove up to 460 watts of heat per canister by the natural convection if the forced ventilation is lost or discontinued. Figure 4-5 provides information on the decay heat from the HLW glass at the designed level of 750 watts of heat at loading [Ref. 4.7]. The figure was extrapolated from 1,000 to 10,000 years.

Failure of the GWSB in the YM EIS No-Action scenario involves a number of failure sequences; these are discussed in the remainder of this section. Table 4-3 summarizes the major failure sequence and Figure 4-6 shows the expected failure in graphic form. This figure does not include damage to the HLW canisters or leaching of the borosilicate glass. The major mechanisms are failure of the weather protection portion of the building and weathering of the concrete floor of the operating area (the cover for the vault) with eventual collapse of the floor.

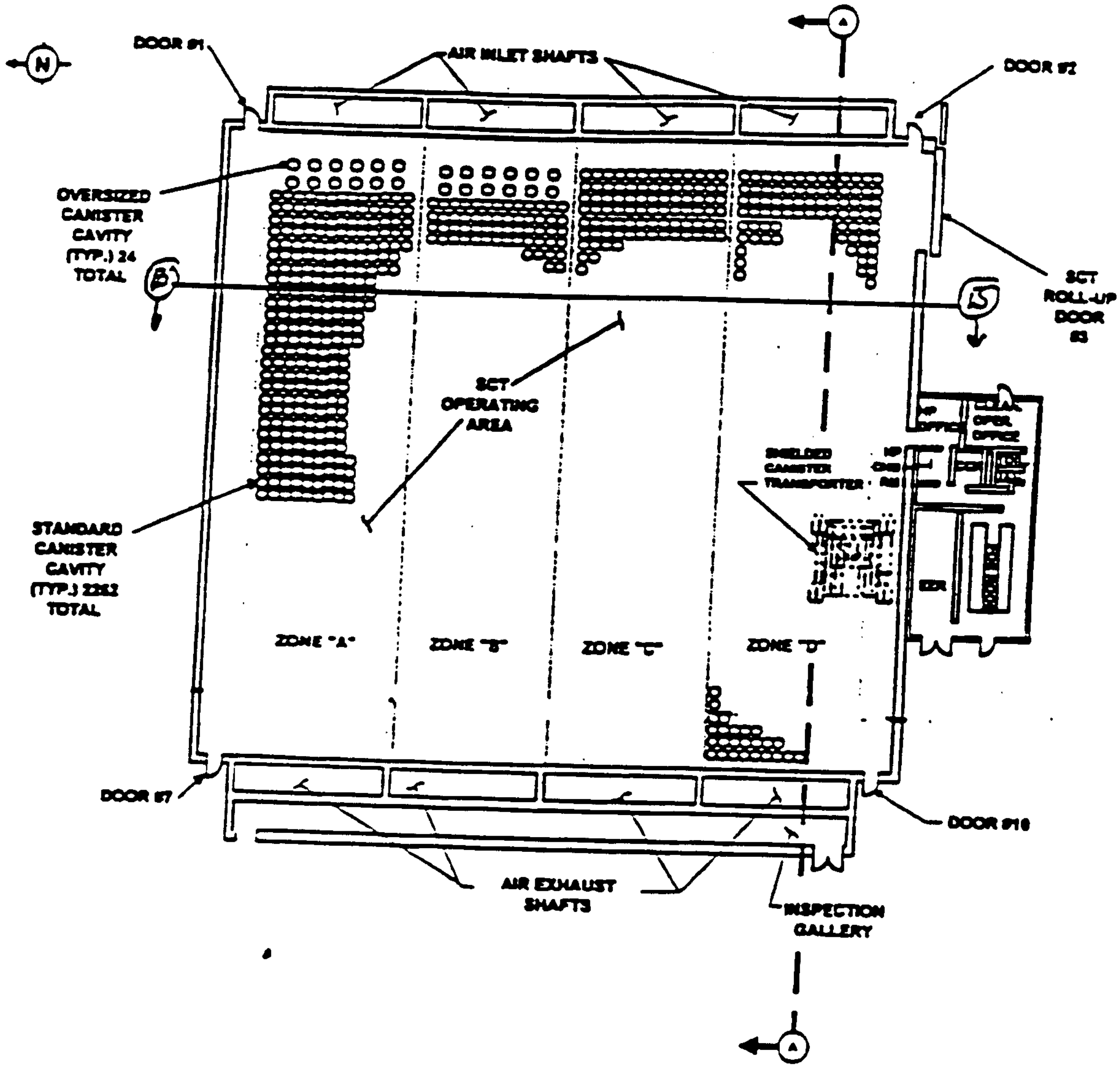

Figure 4-3. General arrangement of glass waste storage building.

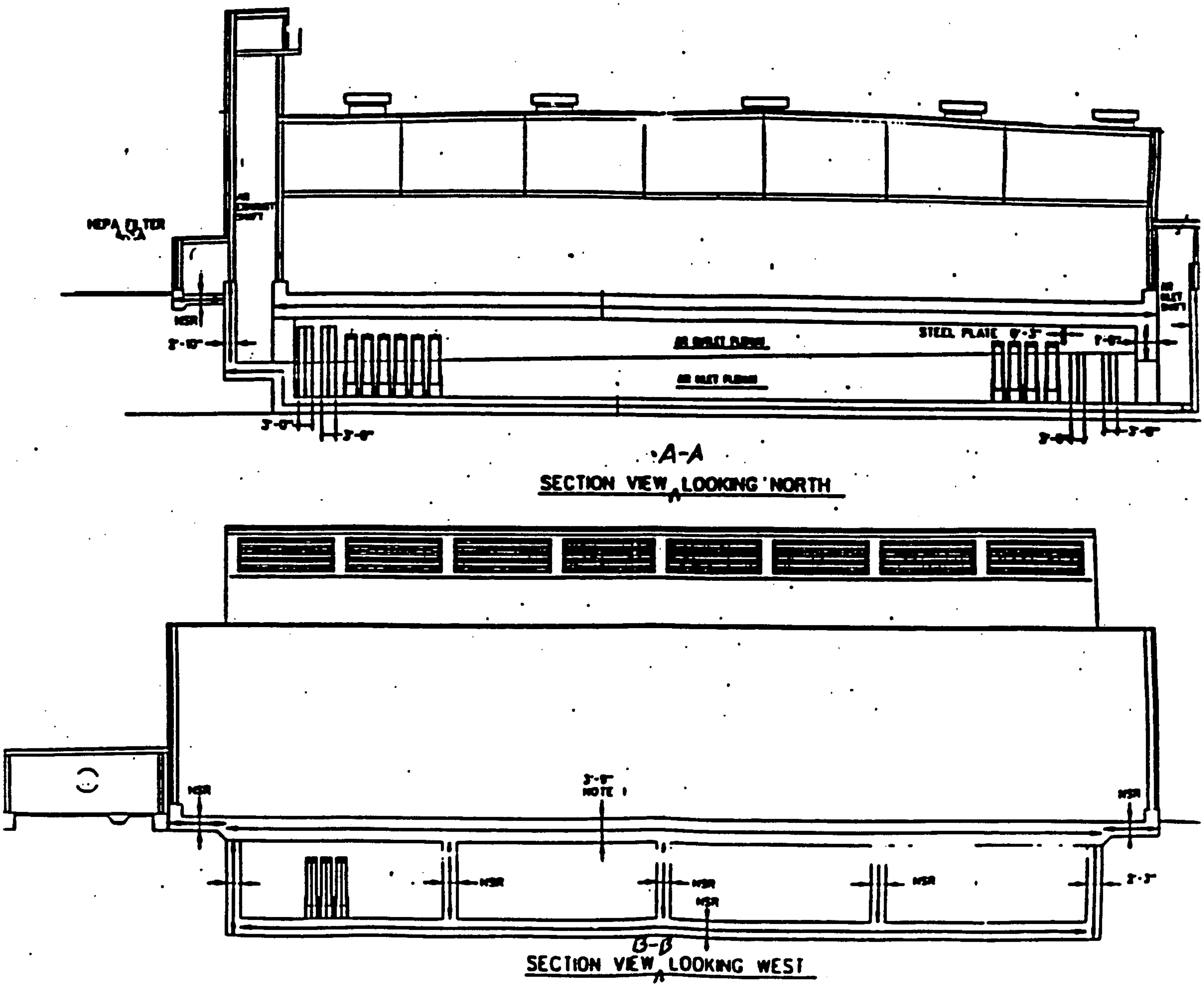

Figure 4-4. Elevation views of glass waste storage building.

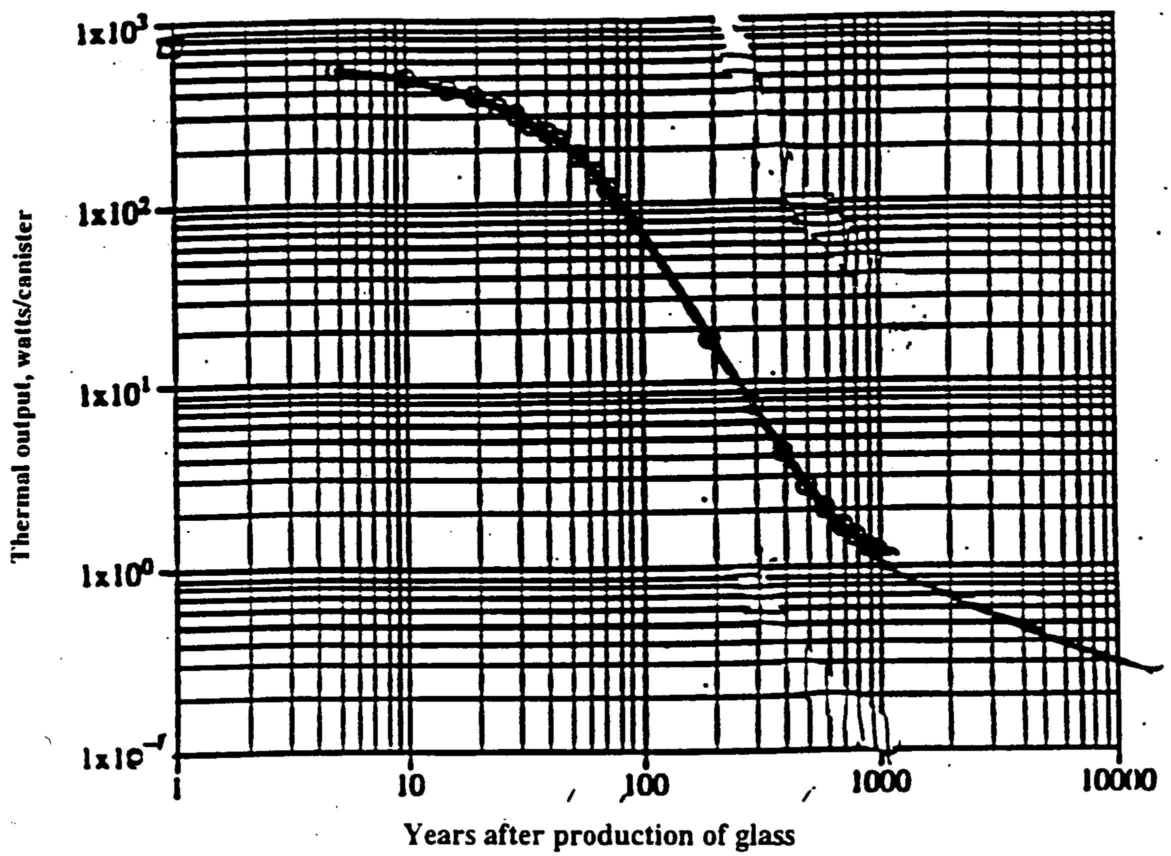

Figure 4-5. Thermal output of HLW design basis glass canister.

Table 4-3. Summary of failure mechanisms and consequences for underground structures at SRS.

Analytical phase	Time frame (years)	Hydraulic conductivity of concrete (cm/sec)	GWSB heat load (kW)	Consequence of failure
Institutional control	0 to 100	1×10^{-10}	160 at 100 years	Power to operate ventilation system shut down at end of period. Natural convection ventilation then cools the vault.
Full protective barrier	100 to 150	1×10^{-10}	69	Weather protection lost at 150 years. After this time, all rain enters vault. Canister heat evaporates water inflow in contact with canisters. Lower section of vault holds water below canister bottom.
Onset of failure of protective barriers	150 to 500	1×10^{-10}	5.5	Heat from HLW continues to evaporate rainfall as described above.
Decreasing protectiveness of barriers	500 to 1,600	1×10^{-7}	1.6	Heat from HLW decreases and rainfall enters vault and overflows to surface. Concrete vault roof continues to weather and surface cracks develop. Shielding plug shoulders weather and fails allowing plugs to begin to fall into vault on top of HLW canisters.
Decreasing protectiveness of barriers	1,600 to 2,500	5×10^{-5}	<1 - heat no longer significant	Seepage of water through walls and floor of vault exceeds annual rainfall and overflow to surface ceases. Radionuclides are released to vadose zone.
Full barrier failure	2,500 to 4,000	1×10^{-4}		Concrete slab from vault roof falls on canisters, breaching storage pipes holding canisters off the floor, and allowing canisters to fall to floor of vault.

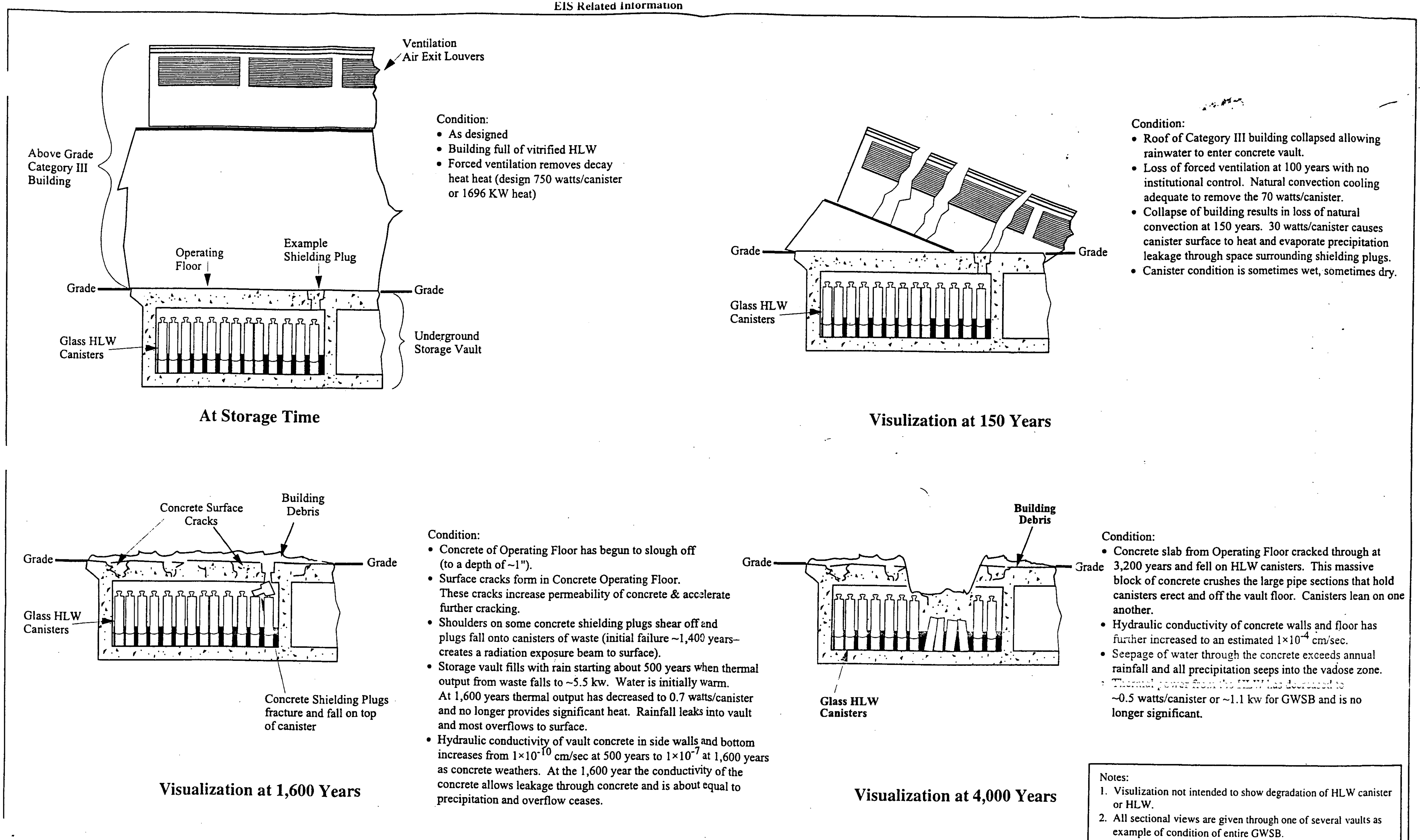

Figure 4-6. Graphical representation of failure of Glass Waste Storage Building (typical of underground storage).

Yucca Mtn/pubsonly/Grfx/4-6 Graphic rep of fail GWSB

4.2.1 WEATHER PROTECTION LOSS AND BUILDING COOLING

This analysis has assumed that the Category III standard constructed weather protection for the GWSB will be maintained during the period of institutional control and will remain in effect for an additional 50 years. The weather protection is assumed to be lost in year 150 and provides no further weather protection. Rain falling on the operating floor of the building leaks through the small gap around each shielding plugs.

The analysis also assumes the forced ventilation is stopped at the end of the institutional control and the GWSB is allowed to use only natural convection cooling. The GWSB is designed for natural cooling and the natural cooling, which was found to add no detrimental effect to this analysis.

4.2.2 CONCRETE DEGRADATION

An analysis of concrete damage shows that the predominate failure mechanism for this underground concrete vault is a combination of physical, chemical, and mechanical forces. Physical and mechanical degradation processes that produce cracking are of primary concern because the concomitant in permeability increases and shielding is potentially lost. The principal chemical processes that may disrupt the integrity of concrete structures are carbonation, calcium hydroxide leaching, and rebar corrosion. Each of these is discussed in Appendix B. Each was evaluated for the operating floor (roof of vault) and the walls and floor of the vault at 1,000 and 10,000 years. (See Table 4-4 for results of this analysis.) The major failure was shown to be cracking and collapse of the operating floor occurring in 3,200 years. Freeze/thaw damage was not evaluated because it was considered a minor consequence for subsurface structures. especially at SRS. It may be more significant at other sites.

Table 4-4. Concrete damage in underground concrete facilities.

	Expected depth of concrete damage	
Degradation mechanism	1,000 years damage	10,000 years damage
Sulfate and magnesium attack	1 cm	5 cm
Carbonation	Reflected in reinforcing bar corrosion	Reflected in reinforcing bar corrosion
Calcium hydroxide leaching	5 cm	23 cm
	Time to cracking of operating floor from stress increases from concrete loss (years)	
Concrete loss	1,600	
	Time to roof collapse (years)	
Reinforcing bar corrosion (average loss of bar cross sectional area at 1,000 year - ~40%)	3,200	

Freeze/thaw damage to the concrete was considered and ruled out as non-significant to degradation of the concrete of this underground facility. Justification for this judgment was based upon the following:

- Most of the concrete is buried underground.
- The concrete slab supporting the Operating Area (roof of the vault), which is 42 inches, is the only concrete that will be exposed to freeze potential.
- The heat generation of the HLW is shown on Figure 4-5.
- Climate at SRS is moderate. Number of days of freezing in Augusta is given in Table 4-2. These freezes are interspersed throughout the 4 winter months and are normally not hard freezes that cause ground freezing. Engineering design specification specify designing to conservative maximum frost depth of 5 inches [Ref. 4.5].
- The sensible heat in the GWSB moderates these periods of freezing.

As a result of these facts, a freeze/thaw analysis was not actually made for this structure. If made, it should show that freeze damage would be slight and affect only the concrete on the surface of the Operating Area concrete which has been treated to resist spalling.

4.2.3 VAULT FLOODING AND LEAKAGE

Analysis of the flooding and leakage potential for this vault shows that the vault goes through periods of thermally hot HLW that evaporates all of rainfall, periods of vault flooding and leakage to the surface of waters from the vault, and periods of seepage through the walls and floor of the basin exceeding rainfall. The thermally hot HLW will evaporate rainfall for the first 1,600 years. By about this time, the decay rate of the HLW has decreased significantly and the continuing aging of the concrete results in increasing hydraulic conductivity. It is expected that by that time, the combination of the two conditions results in no further overflow from the basin, which drains over time as the concrete continues to weather. The expected hydraulic conductivity of the concrete and the thermal load from the HLW are given in Table 4-3.

4.2.4 EXPOSURE OF PEOPLE TO DIRECT RADIATION FROM HLW

The analysis concludes that people in the vicinity of the GWSB will be exposed to direct radiation from HLW from failure of the vault integrity starting at 1,400 years when the shielding plugs begin to fail and drop into the vault. Much more severe exposure and possible contact of the HLW will occur when the roof collapses. This was determined to be at 3,200 years.

4.3 Underground Structures in Arid-Xeric Environment

This section evaluates differences that might be expected from locating the GWSB at the Hanford Site or other locations considered to be arid-xeric environment. In an arid-xeric environment, the evaporative capacity far exceeds the precipitation. At Hanford, the evaporative capacity is approximately seven times the precipitation rate [Refs. 4.5 and 4.8]. The lack of rainfall is complicated by the fact that about 50% of the precipitation occurs during the 4 winter months (November through February) [Ref. 4.9]. The deficit in precipitation is caused largely by the rain shadow created by the Cascade Mountains and results in the arid-xeric environment. The normal rate of precipitation is low and, as defined in Reference 3.4, less than 3% of the precipitation results in run off. Most of the remainder is lost through evapotranspiration. Figure 4-7 shows the comparison between precipitation rates at SRS and Hanford environments. SRS's precipitation rate is defined as a humid-mesic environment and Hanford as an arid-mesic environment.

The main difference for underground waste storage at SRS and Hanford is precipitation rates. Hanford's precipitation rate during the wet winter months is still one quarter that of SRS and one tenth that of SRS's precipitation rates during the remainder of the year. Table 4-5 summarizes the consequence of storage of waste in a facility similar to the GWSB located at Hanford.

4.4 Extrapolation to Other Points in the United States

Figures 4-8 and 4-9, obtained from Reference 4.5, provide information on national precipitation (Figure 4-8) and evaporation potential (Figure 4-9). Used in combination, these two figures provide information that can be used to show regional weather patterns. The reader can estimate which scenario (that described in Section 4.2 for a humid-mesic or Section 4.3 for an arid-xeric) may apply to underground storage of SNF and HLW. This same information may be used for surface storage. This information, when used with site-specific precipitation (rainfall and frozen precipitation) data, should allow reasonable failure scenario evaluation for commercial reactors located throughout the United States.

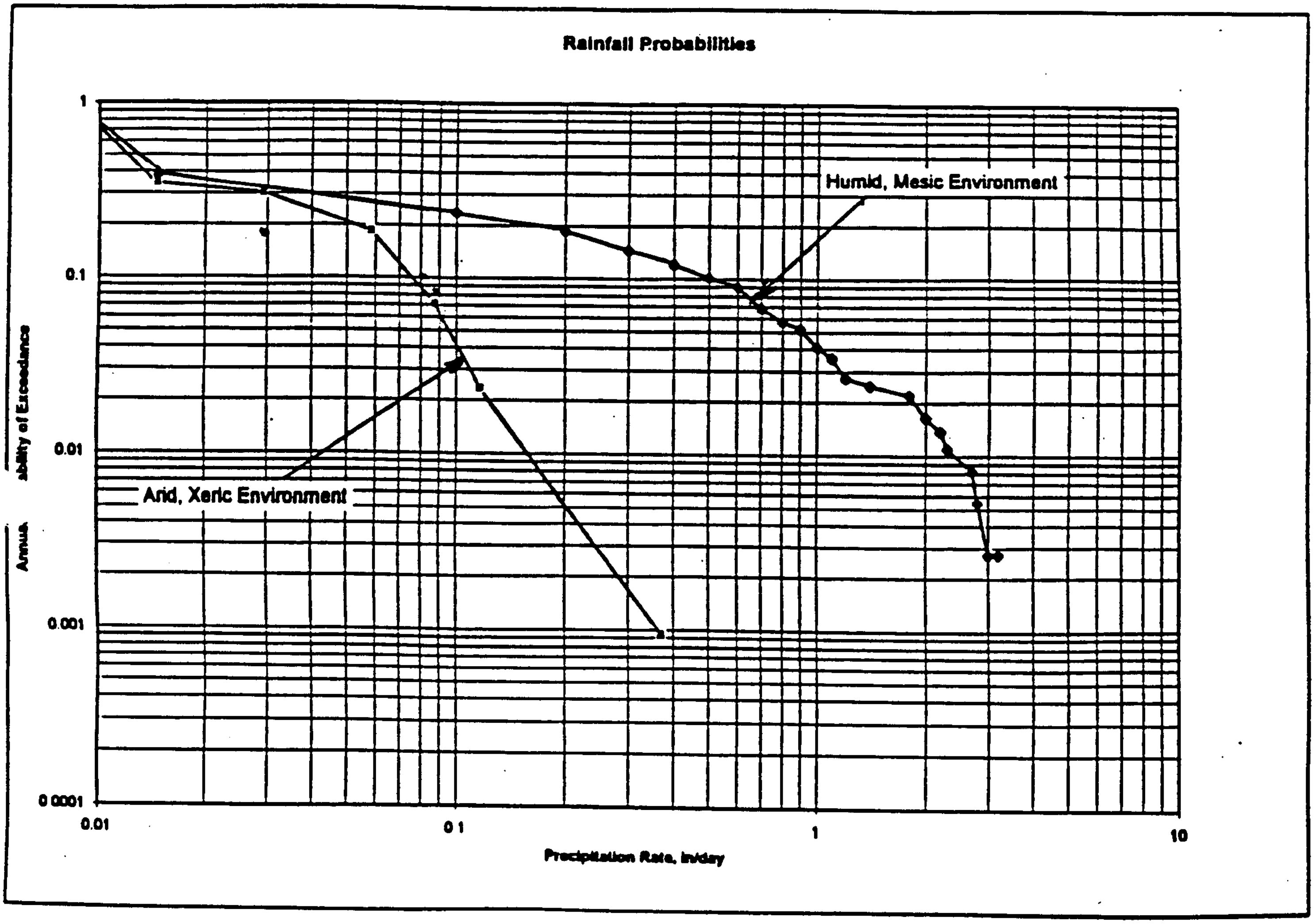

Figure 4-7. Typical precipitation probabilities in arid-xeric and humid-mesic environments.

Table 4-5. Summary of failure mechanisms and consequences for underground structures at Hanford.

Analytical phase	Time frame (years)	Hydraulic conductivity of concrete (cm/sec)	GWSB heat load (kW)	Consequence of failure
Institutional control	0 to 100	1×10^{-10}	160 at 100 years	Power to operate ventilation system shut down at end of period. Natural convection ventilation then cools the vault.
Full protective barrier	100 to 150	1×10^{-10}	69	Weather protection lost at 150 years. After this time all precipitation enters vault. Canister heat evaporates water inflow in contact with canisters. Water puddles in lower section of vault and evaporates due to dry ambient atmosphere at Hanford.
Onset of failure of protective barriers	150 to 500	1×10^{-10}	5.5	Heat from HLW decreased: precipitation continues to enter vault and evaporates. During this time vault environment cycles between humid and arid conditions.
Decreasing protectiveness of barriers	500 to 900	1×10^{-7}	1.6	Precipitation continues to enter vault and evaporate. Concrete vault roof continues to weather and surface cracks develop. Shielding plug shoulders weather and fail allowing plugs to begin to fall into vault on top of the HLW canisters.
Decreasing protectiveness of barriers	900 to 1,600	5×10^{-6}	1.5	Seepage of water into the concrete walls and floor of vault occurs during periods of precipitation. This water permeates the concrete barriers and transports radionuclides with it to the vadose zone. During prolonged dry periods, water evaporates from the concrete. As the water evaporates, the radionuclides are left in the concrete.
Decreasing protectiveness of barriers	1,600 to 2,500	5×10^{-5}	<1 - heat no longer significant	Seepage of water into the concrete walls and floor of vault occurs during periods of precipitation. This water permeates the concrete barriers and transports radionuclides with it to the vadose zone. During prolonged dry periods, water evaporates from the concrete. As the water evaporates, the radionuclides are left in the concrete.
Full barrier failure	2,500 to 4,000	1×10^{-4}		Concrete slab from vault roof fall on top of canisters breaching storage pipes holding canisters off the floor allowing canisters to fall to floor of vault.

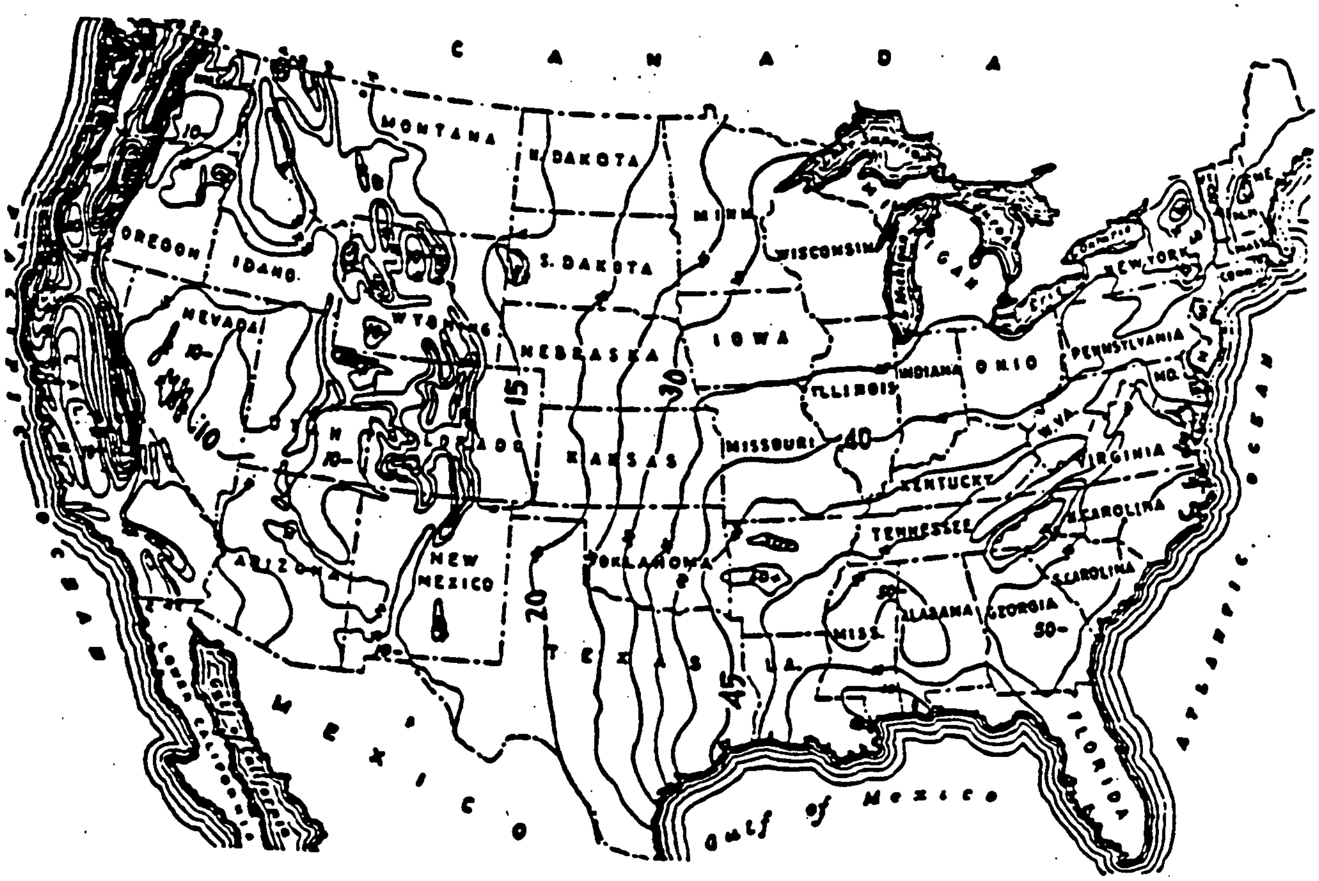

Figure 4-8. Annual precipitation rates for all regions of the contiguous United States, inches precipitation per year.

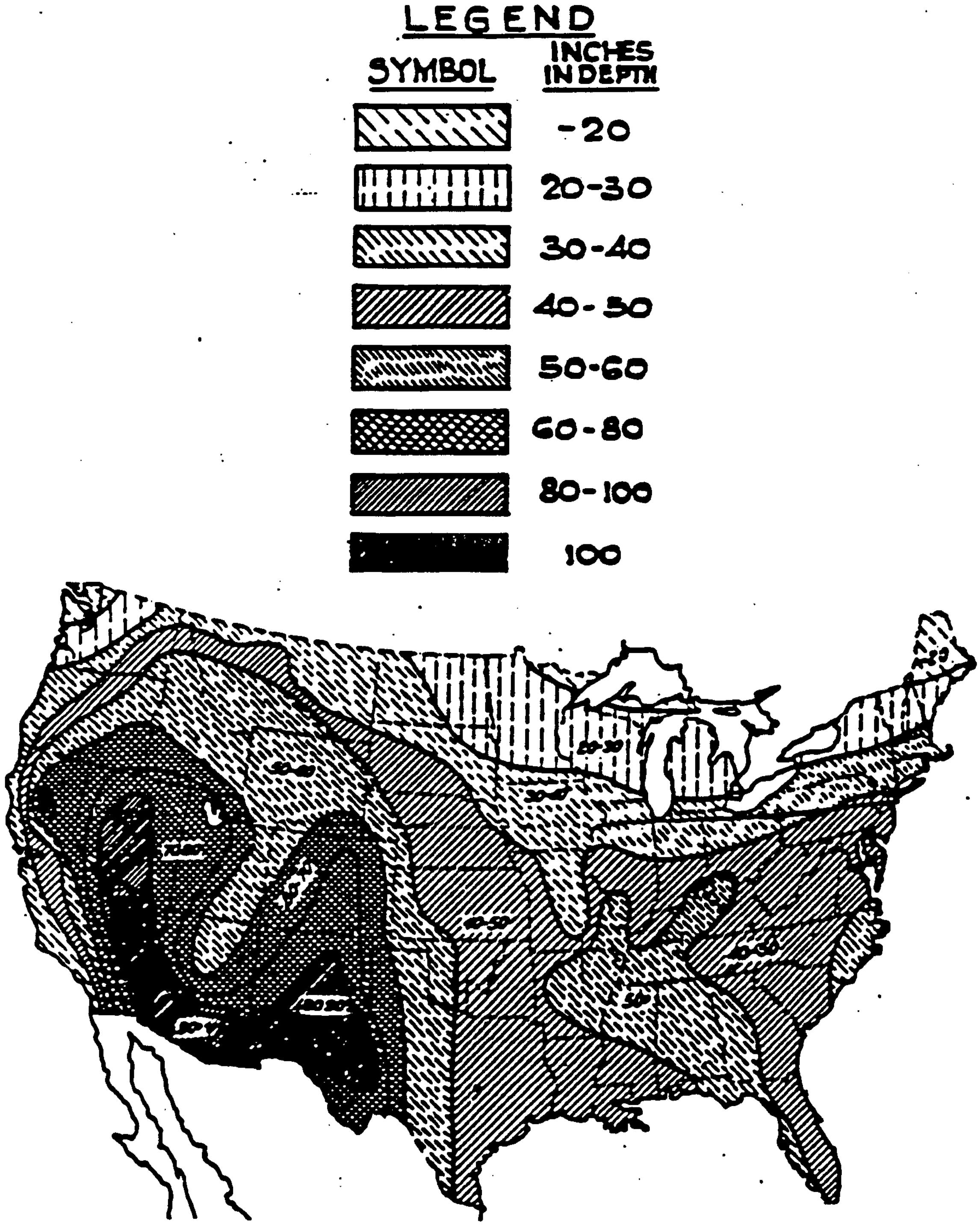

Figure 4-9. Annual evaporation rates for all regions of the contiguous United States, inches precipitation per year.

4.5. Section 4 References

4.1 Fetter, Jr., C. W., 1980, *Applied Hydrology*, University of Wisconsin, Oshkosh, Charles E. Merrill Publishing Company.

4.2 National Climatic Data Center, 1996, *Local Climatological Data -- Annual Summary with Comparative Data*, Asheville, North Carolina.

4.3 Poe, W. L., and Wise, P. F., 1998, *National Weather Affecting Long-Term Degradation of Commercial Spent Nuclear Fuel and DOE Spent Nuclear Fuel and High-Level Waste*, Tetra Tech-NUS, Inc., Aiken, South Carolina, October.

4.4 DOE (U.S. Department of Energy), 1997, *Environmental Impact Statement - Accelerator Production of Tritium at the Savannah River Site*, DOE/EIS-0270D, December.

4.5 Seelye, E. E., 1968. *Design*, Text book for Civil Engineers, Printed by John Wiley and Sons, Inc., New York, New York.

4.6 Parsons, A. M., and M. M. Gruebel, 1996, *Hydrology of the F-Area at the Savannah River Site*, March.

4.7 WSRC (Westinghouse Savannah River Company), 1996, *Defense Waste Processing Facility - System Design Description - Glass Waste Storage Building - Structure and Services, CS-01*, Document Number G-SYD-S-00068, Revision 1, June.

4.8 Hoitink, D. J. and K. W. Burk, 1997, *Hanford Site - Climatological Data Summary 1996 - With Historical Data*, Document PNNL -11471, Pacific Northwest National Laboratory, Richland, Washington, April.

4.9 Garvin, L. G., 1997, *Canister Storage Building (CSB) Report Phase 3: Safety Analysis Documentation Supporting CSB Construction*, Document Number HNF-SD-SNF-RPT-004, Revision 7A, August.

APPENDIX A. NUHOMS SURFACE STORAGE FACILITY DEGRADATION ANALYSIS

(Information in this Appendix has been adapted from Reference 1.2, Appendix D)

The information contained in this appendix summarizes the information on concrete degradation contained in Reference 1.2, Appendix D. The information was used in the NUHOMS SER to show that exposure to the natural environment during the 50-year design life of the NUHOMS HSM would not present undue risk to the workers, the public, or the environment. This assumption is included in the long-term degradation report as the starting point for long-term degradation of this concrete storage module.

The effects of short- and long-term elevated temperatures on concrete structures have been a subject of much research in the U.S. and European communities, and findings of these studies and tests are documented. A number of these publications and test reports, particularly those in References A.1 through A.10, were searched for characteristics of concrete under sustained elevated temperatures. This report describes concrete characteristics as they relate to physical/chemical reactions and subsequent effects on mechanical properties.

Changes in concrete properties under elevated temperatures and under atmospheric pressure are primarily attributable to the loss of free water. In ordinary saturated concrete, 2% to 10% of the volume is occupied by evaporable free water. Upon heating, a portion or all of this water could be removed. Lankard et al. [Ref. A.4] identified five types of evaporable free water that differ in the degree of attraction to the solid materials present as follows:

- Water in capillary pores
- Water in gel pores
- Water absorbed on crystal surfaces
- Adsorbed water confined between adjacent crystal surfaces
- Zeolitic intracrystalline water

When concrete is subjected to elevated temperatures, the free water would be removed in approximately the order listed above (i.e., capillary) and large pore water would be the first to come off, gel waters next, and so on. At a temperature of 175°F, some of the capillary water will be lost; however, hydration of cement will continue. R. D. Allen [Ref. A.5] reports that the capillary water is evaporated and released by heating to 100°C (211°F), but the loss of adsorbed water occurs over a broader temperature range, with all evaporable water driven off by 300°C (572°F). At this temperature the microstructures change.

Degradation or deterioration of concrete as it relates to greater crack formation and subsequent spalling is generally attributed to the loss of chemically combined or nonevaporable water. Lankard et al. [Ref. A.4] reports that the results of tests on unsealed concrete specimens indicate: "An increase in chemically combined water content of the cement phase at 175°F and 10, 20, 40 percent loss of this water at 250, 375, and 500°F, respectively." The loss of chemically combined water will cause dehydration of concrete. R. D. Allen concludes that the principle dehydration reactions are:

- Decomposition of cement gel into dicalcium silicate, beta wallastanite, and water
- Decomposition of calcium hydroxide into lime and water

The actual effect of this dehydration reaction is weakening of the bond between cement gel phases, which in turn affects its mechanical strength and may cause microcrack formation and shrinkage of the cement. It is interesting to note that these dehydration reactions with reduced strength phases are reversible if water is reintroduced into the concrete.

From the above observation and given the fact that the NUHOMS-24P HSMs concrete will not reach temperatures beyond 197°F for the maximum summer average ambient temperature of 100°F, it can be concluded that no adverse effect as it relates to degradation or deterioration of concrete can be anticipated under normal storage conditions. The adequacy of the HSM concrete is further substantiated by the fact that the maximum concrete temperature of 144°F for the lifetime average ambient temperature of 70°F is below ACI 349-85 Code, Paragraph A.4.1 long term temperature, limit of 150°F. Indeed, the maximum HSM concrete temperatures for the 100°F ambient temperature case are below the 150°F temperature limit at all module locations except the local areas near the center of the roof and floor slabs, which are well within the ACI 349-85 Code, Paragraph A.4.1 local temperature limit of 200°F.

The physical changes (i.e., loss of evaporable water) and also the chemical changes (i.e., dehydration and formation of other hydrated cement phase associated with loss of nonevaporable or chemically combined water at sustained elevated temperatures) will affect concrete mechanical properties. Mechanical properties most affected by elevated temperatures are compressive strength, modulus of elasticity, tensile strength, Poisson ratio, and creep. In recent years extensive testing of concrete mechanical properties at elevated short- and long-term temperatures have been performed and published. The results of the majority of these tests indicate that compressive strength of sample specimens heated up to (and occasionally above) 250°F and exposed to ambient humidities have changed very little, and frequently exhibit an increase in strength when compared to similar samples stored at room temperature.

Based on the results of tests performed, V. V. Bertero and M. Polvika [Ref. A.6] report that: "If the free moisture is allowed to escape during heating to 300°F, the mechanical characteristics of the concrete are very little affected by the heat treatment. This is true regardless of the number of cycles or duration of the thermal treatment." Other tests which include long-term effects have also reached similar conclusions. K. W. Nasser [Ref. A.7] concludes from year-long tests performed on 500 specimens in a temperature range of 70°F to 205°F that the gain in strength beyond the age of 14 days increases with temperature (Figure A-1). In another test performed by Construction Technology Laboratories, Portland Cement Association [Ref. A.8] on Hanford concrete, specimens were tested at temperatures of 250°F, 350°F, and 450°F for durations as long as 920 days. The results of these tests further verify the above conclusion. It is interesting to note that even at 450°F the concrete compressive strength did not fall below the original mix designs of 4,500 psi and 3,500 psi (Figure A-2).

In general, the increase in compressive strength at moderate elevated temperatures (below 250°F) is attributable to the removal of the evaporable water. Other tests performed by M. S. Abrams [Ref. A.3], A. Weber et al. [Ref. A.10], Kanazu et al. [Ref. A.9], and a number of other tests have all indicated similar findings that the concrete compressive strength is little affected by elevated temperatures up to 250°F. At temperatures above 250°F, concrete begins to lose some strength. This is attributed to the chemical changes (i.e., dehydration) that occur in the cement phase as described earlier.

For the purpose of design, the NUHOMS-24P HSM concrete strength was very conservatively reduced by 10% at 400°F for all normal, off-normal, and accident load combinations. This reduction is based on the curves presented by M. Fintel [Ref. A.2] as shown in Figure A-3. Other mechanical properties that

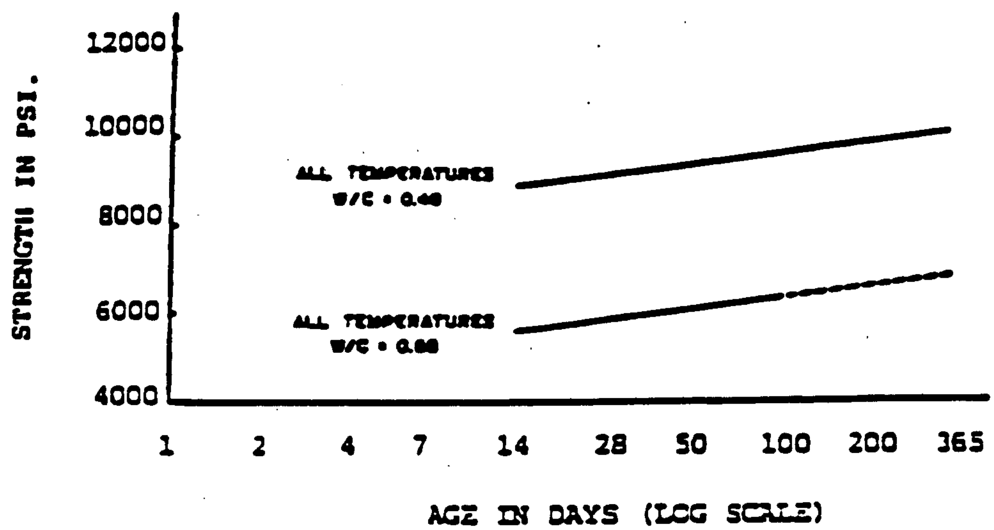

Figure A-1. Concrete strength versus time at water to concrete ratios of 0.40 and 0.60 good for temperatures to 205°F.

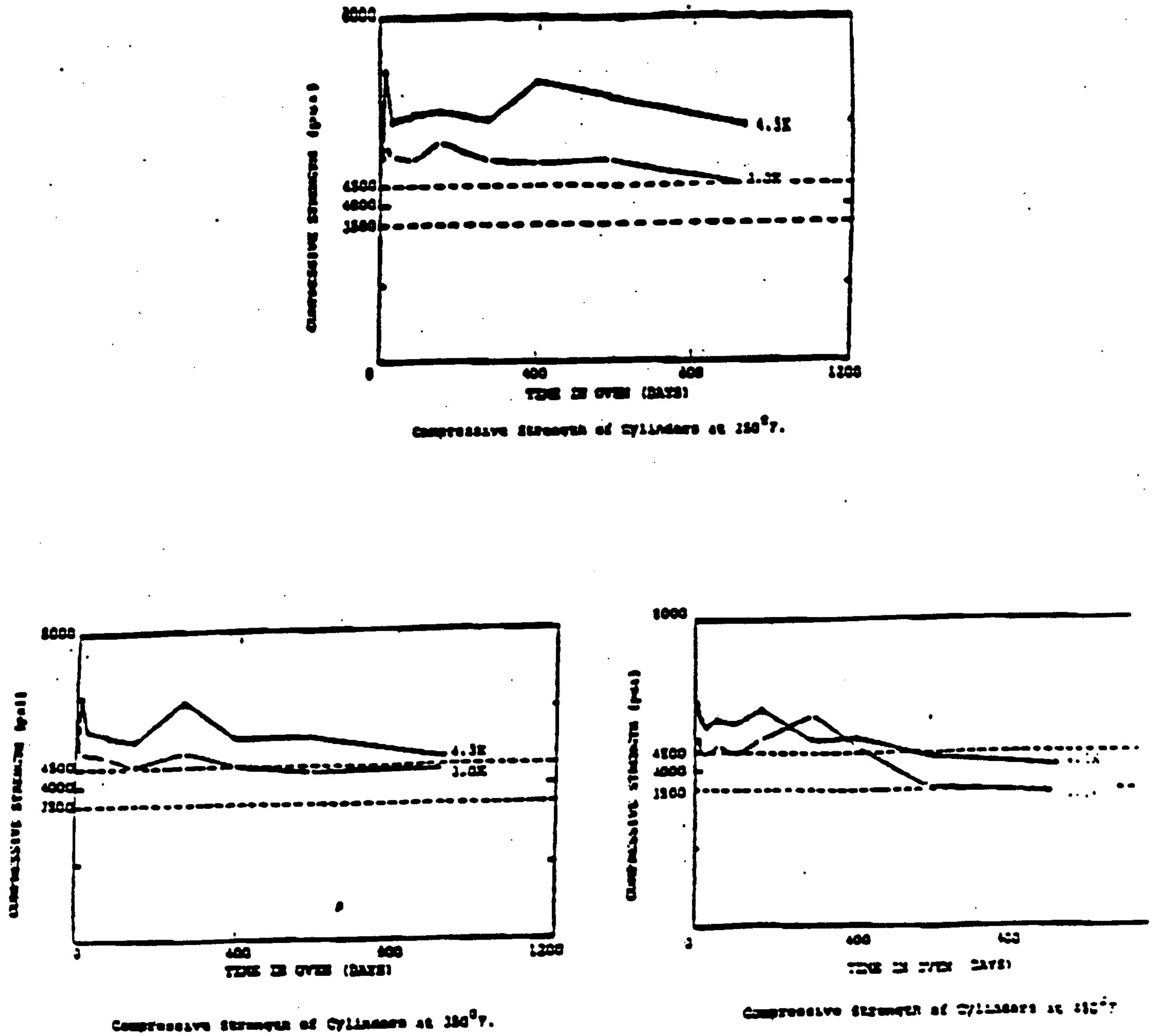

Figure A-2. Concrete compressive strength at 250°, 350°, and 450°F.

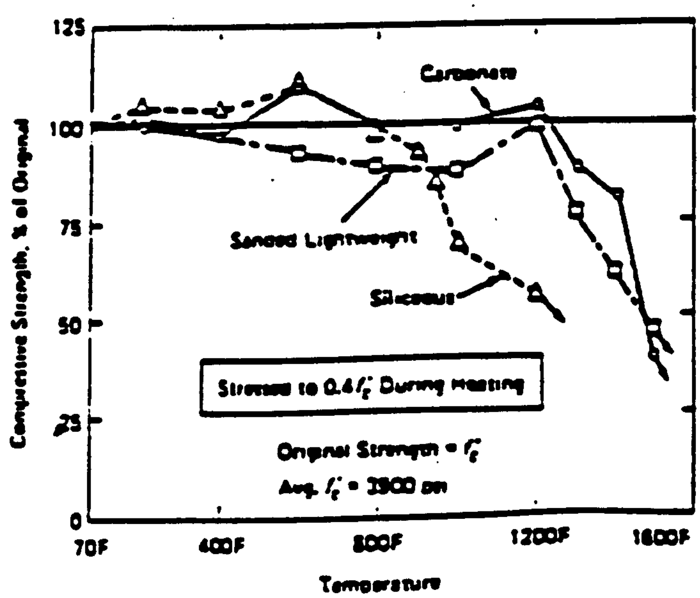

Figure A-3. Temperature effect on concrete.

are affected by elevated concrete temperatures are tensile strength and modulus of elasticity. Since the design of NUHOMS does not rely on the tensile strength of concrete due to the use of reinforcement, loss of this strength under elevated temperatures will not affect the NUHOMS design. The reinforcing bar tensile strength, however, was conservatively selected at 400°F for all normal, off-normal, and accident load combinations.

The modulus of elasticity also decreases with the increased temperature of concrete. Again, the loss of water explains the reduction in modulus of elasticity. According to Lankard, the absence of free water in heated concrete means that more concrete occupies the same volume with the added strength of the concrete. As shown in Figure A-4, the loss in the modulus of elasticity due to elevated temperatures up to 200°F is expected to be approximately 10% of the original value. The modules of from the flexural rigidity of the structure simultaneously affect the magnitude of the thermal stresses induced under constrained conditions. A substantial reduction in this property will cause excessive flexural deformation in long span beams. Since the NUHOMS walls and roof slabs are deep, short span members, the added deflections in these members under 10% loss of modulus of elasticity is considered negligible.

Other mechanical properties such as creep and Poisson ratio were also considered and their effects under elevated temperatures investigated and found to have insignificant impact on the design of the NUHOMS modules. Although the loss in the concrete's modulus of elasticity will decrease the thermal stresses, this loss was not considered in the design of HSMs for sake of conservatism.

In conclusion, given the maximum concrete design temperatures of the NUHOMS-24P HSMs (i.e., less than 150°F for the 70°F lifetime normal ambient case and less than 200°F for the maximum normal summer ambient case of 100°F), the concrete integrity is unaffected and is in compliance with the ACI 349-85 Code. In addition, the maximum HSM concrete temperature of 215°F for the 125°F short-term extreme ambient temperature case are well within the ACI 349-85 Code, Paragraph A.4.2 short-term temperature of 350°F. The same can be said for the worst case accident condition with the HSM vents assumed to be blocked with an extreme ambient temperature of 125°F for which the maximum HSM concrete temperatures are less than 350°F, except at localized areas near the center of the roof and floor slab. At these locations, the maximum concrete temperatures are 368°F and 395°F, respectively, which are well below the ACI 349-85 Code, Paragraph A.4.2 short-term local temperature limit of 650°F. It is also noted that the average temperatures through the thickness of the roof and floor slabs are less than 300°F for this worst case. Therefore, the NUHOMS-24P HSM design is in full compliance with the ACI 349-85 Code requirements. Nevertheless, the concrete compressive strength and rebar yield of 20.7 ksi at 400°F were used in calculating the concrete section capacities for the 125° extreme off-normal and accident load cases to provide a conservative result. The conservatism on the concrete properties and temperatures that meet the ACI 349-85 requirements eliminates the need for surveillance inspection of the interior concrete surfaces following DSC emplacement.

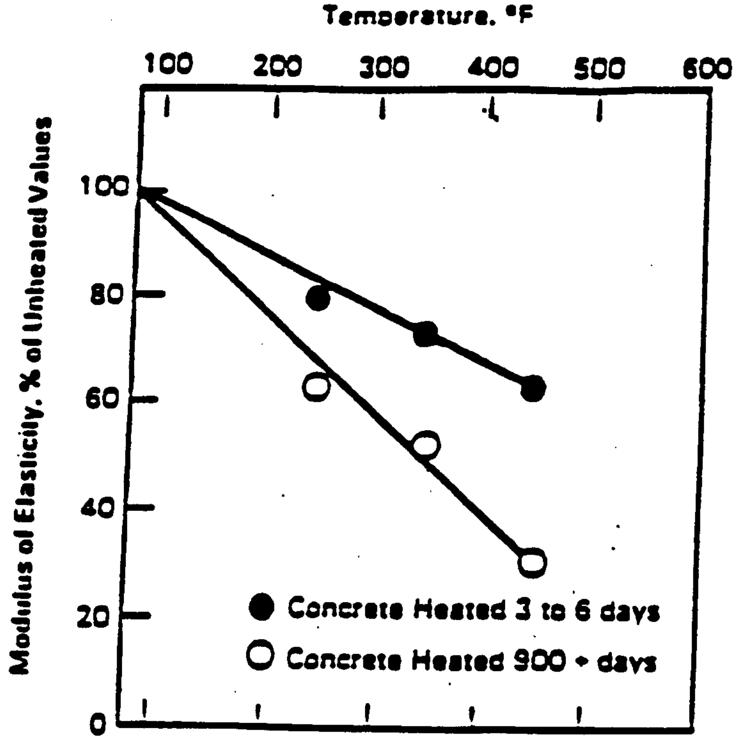

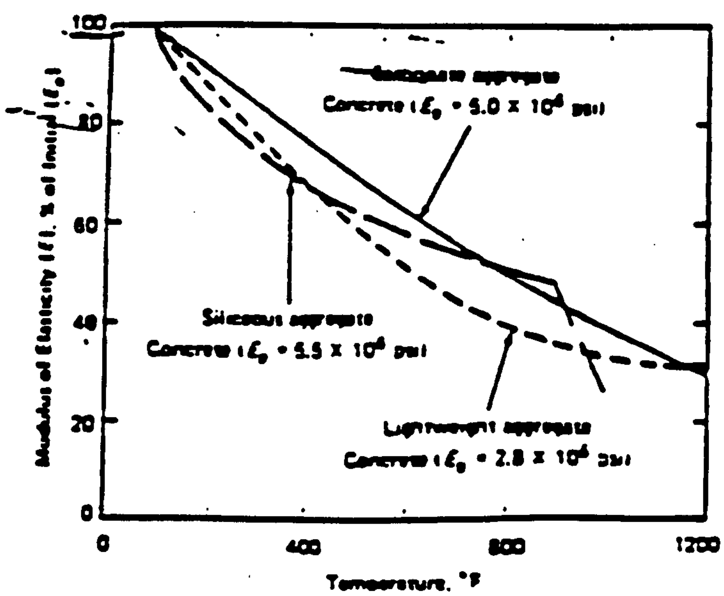

Figure A-4. Modulus of elasticity of concrete at high temperatures.

Appendix A References

A.1 Zoldners, N. G., 1970, *Thermal Properties of Concrete Under Sustained Elevated Temperatures*, ACI Publication, paper SP25-1, American Concrete Institute, Detroit, Michigan.

A.2 Fintel, M., 1974, *Handbook of Concrete Engineering*, Van Nostrand Reinhold Co., New York, New York.

A.3 Abrams, M. S., M. P. Gillen, and D. H. Campbell, 1970, *Elastic and Strength Properties of Hanford Concrete Mixes at Room and Elevated Temperatures*, Construction Technologies Laboratories, Portland Cement Association, Skokie, Illinois.

A.4 Lankard, D. R., et al., 1970, *Effects of Moisture Content on the Structural Properties of Portland Cement Concrete Exposed to Temperatures Up to 500°F*, ACI Special Publication, SP25, American Concrete Institute, Detroit, Michigan.

A.5 Allen, R. D., 1984, *High Temperature Properties of Concrete Relevant to Monitored Retrievable Storage Application*, Battelle, Pacific Northwest Laboratories.

A.6 Bertero, V. V., and M. Polvika, 1972, *Influence of Thermal Exposures on Mechanical Characteristics of Concrete*, ACI Special Publication, SP.34, Concrete for Nuclear Reactors, Volume 1, American Concrete Institute, Detroit, Michigan.

A.7 Nasser, K. W., 1970, *Creep of Concrete at Low Stress Strength Ratios and Elevated Temperatures*, ACI Special Publication SP25, American Concrete Institute, Detroit, Michigan.

A.8 Rockwell International, *Effect of Long-Term Exposure to Elevated Temperature on the Mechanical Properties of Hanford Concrete*, Construction Technology Laboratories, Portland Cement Association Report RHO-C-54.

A.9 Kanazu, T., et al., 1985, *Mechanical Behavior of Concrete and Reinforced Concrete at Elevated Temperature Up to 500°C*, Transactions of the 8th International Conference on Structural Mechanics in Reactor Technology (SMIRT), Volume H, North-Holland for CEC.

A.10 Weber, A., and G. Becker, 1985, *Effects of Long Term Exposure on the Behavior of HTR Concrete*, Transactions of the 8th International Conference on Structural Mechanics in Reactor Technology, Volume H, North-Holland for CEC.

APPENDIX B. E-AREA VAULTS UNDERGROUND STORAGE FACILITY ENGINEERED BARRIER DEGRADATION AND FAILURE

(Information in this Appendix has been adapted from Reference 3.1)

The concrete degradation description in this appendix was adapted from a performance assessment of SRS Low-Level Waste disposal in the E-Area Vaults. The design of these E-Area vaults and the GWSB are not identical but have many of the same features that may cause degradation of the GWSB. The E-Area vaults and the GWSB both have unsupported reinforced concrete roof, reinforced concrete side walls and floors. The major failure consequence is associated with collapse of the concrete roofs. This appendix summarizes information obtained from Reference 3.1 as it can be used in the failure analysis for the GWSB. The E-Area vaults unsupported concrete roofs are 15 meters wide and 8.8 meters high. The normal grade is at about the top of the vault. Figure B-1 shows a typical section through one of these vaults. DOE plans to cover the vaults with an RCRA-type cover when filled. Figure B-2 shows the expected RCRA cover that will be placed on top of these vaults. Three types of structures, Intermediate Level Tritium Vaults (ILT), Intermediate Level Non-Tritium Vaults (ILNT), and Low Activity Waste Vaults (LAW), are analyzed in this performance analysis. Each have slightly different designs and physical dimensions but are evaluated in the same manner that is discussed in the remainder of the appendix.

The following two sections address degradation of the engineered cover and the concrete vaults. Degradation of the cover is addressed first. The GWSB is not expected to have an engineered cover so the information is presented here for background on the failure discussion of the concrete E-Area vaults, which are similar to the GWSB. In general, cover degradation is considered in a binary fashion (i.e., it is assumed to be functional or it is assumed to be nonfunctional). Vault degradation is addressed in the second section. The primary mode of vault degradation is expected to be cracking and eventual failure of the roof.

B.1 Cover Degradation

Degradation of the cover is expected to occur by a number of processes. Potential processes are erosion; penetration by plants and animals; external events such as settling or slumping or a seismic event; and human intrusion. These processes will reduce the effectiveness of the cover to limit the vertical moisture flux. Over the period of analysis, the net flux through the cover is expected to approach the background levels for the site, (i.e., 40 cm/year).

As presently conceived in the closure concept, shallow-rooted bamboo will be planted on the disposal site and a system of drainage ditches will be constructed to handle surface runoff and diverted infiltration. As specified in DOE Order 5820.2A, active institutional control is assumed for only 100 years. During this time, periodic site inspection would reveal any degradation of the overlying cover and drainage system and corrective actions would be taken. Cover degradation during this first 100 years is likely to be minimal. Sheet erosion will occur, but the bamboo vegetative cover would minimize the effects of this disturbance. Erosion is reduced several hundred fold if a dense vegetative cover is present. This suggests that there will be little erosion as long as the bamboo vegetative layer has not been cleared; however, the cover may be eroded down to the gravel layer in as little as 800 years after the bamboo vegetative layer is cleared. However, erosion of the gravel layer is difficult to predict. In this analysis, it is assumed that the cover remains functional until the roof of the vault fails and thus, no longer provides support for the cover.

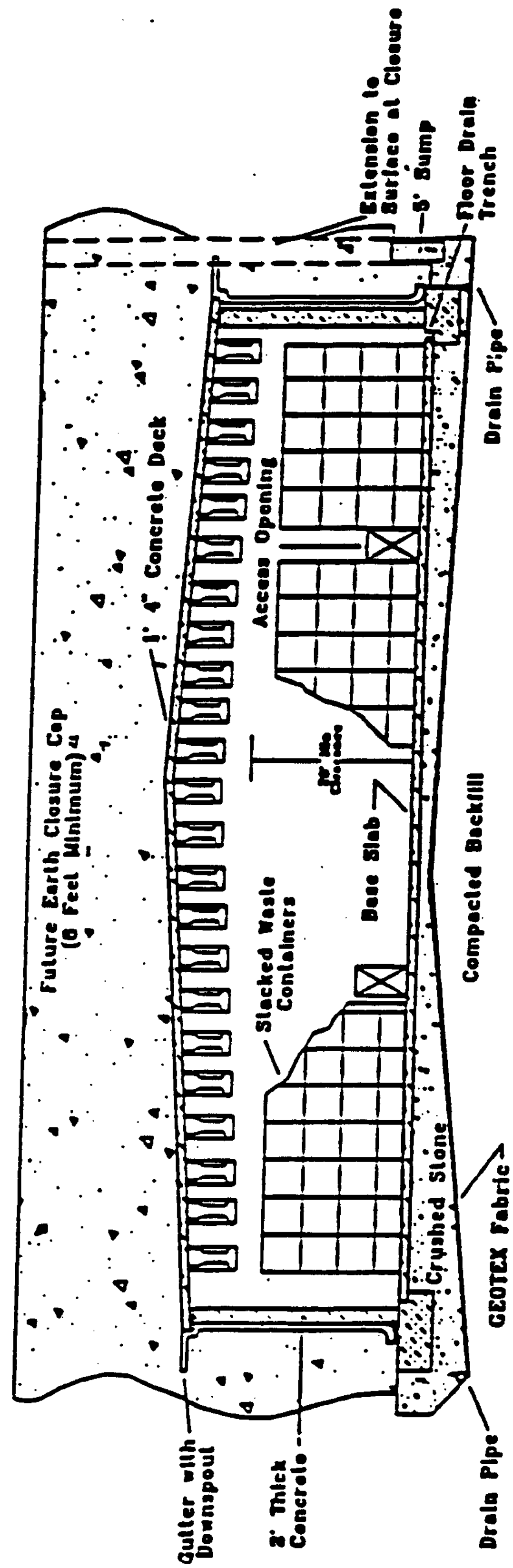

Figure B-1. Typical section through Low Activity Waste Vault cell.

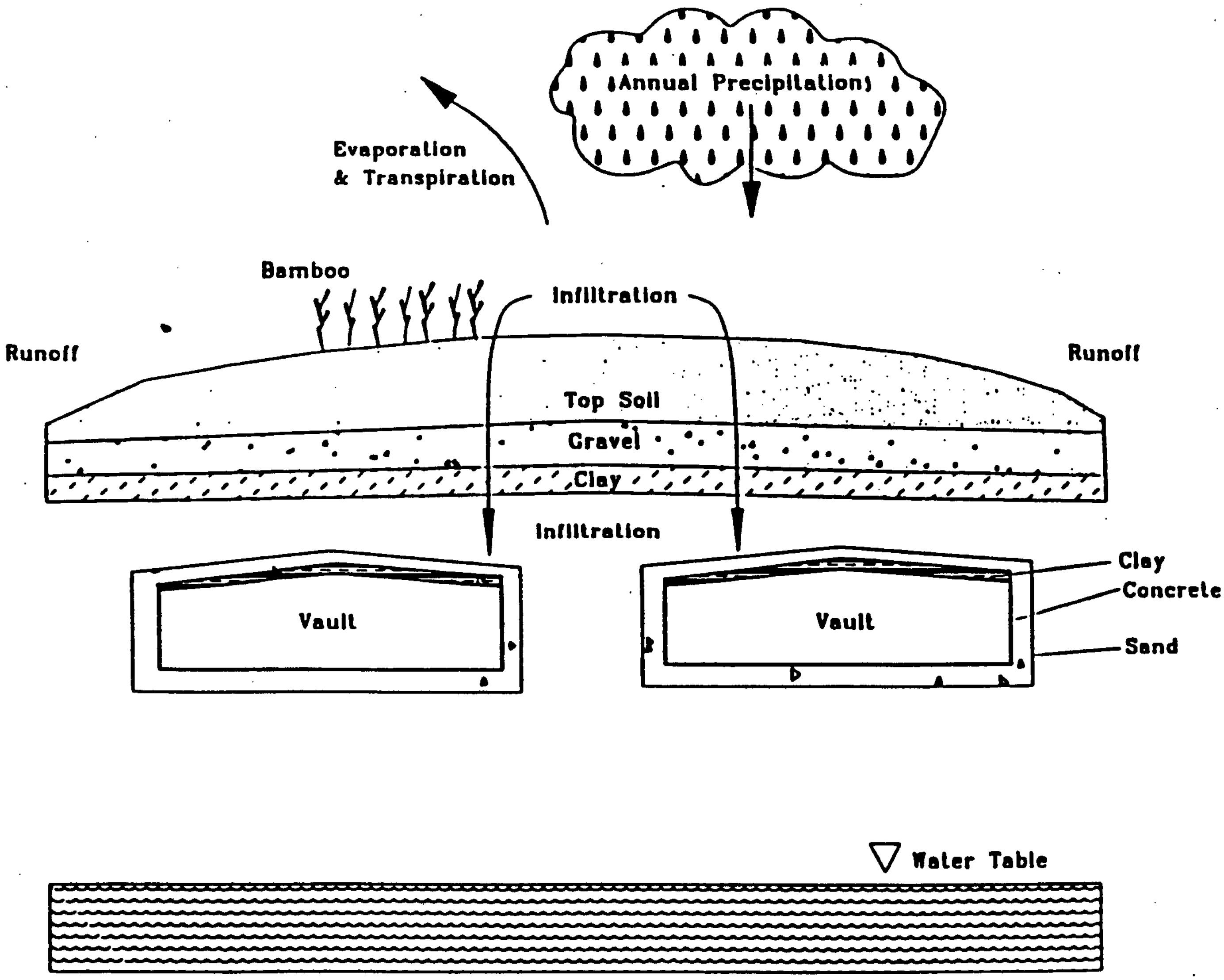

Figure B-2. Low Activity Waste Vault closure concept.
(2 cm/year infiltration)

B.2 Vault Degradation

The concrete vaults are expected to degrade slowly through a combination of physical, chemical, and mechanical processes [Ref. B.1]. Physical and mechanical degradation processes that produce cracking are of primary concern because of permeability increases. Shrinkage cracks occur as a result of the temperature cycling during curing of concrete structures, and thus are present before the facility closure cover is constructed. This allows for filling the outer portion of the cracks, in the vault walls or roof, with epoxy prior to closure. Cracking might occur after the vaults have been covered as a result of degradation of the epoxy used to fill shrinkage cracks, foundation settling, or rebar expansion due to corrosion.

The principal chemical processes that disrupt the integrity of concrete structures are sulfate attack, carbonation, calcium hydroxide leaching, and rebar corrosion. The effects of these processes on E-Area Vault degradation have been analyzed using the methodology described in Walton et al. [Ref. B.1]). The methodology quantifies the extent of concrete degradation in terms of the penetration depth. The depth is the amount of thickness that has degraded. A brief discussion of the mechanisms affecting vault durability are provided in the following sections.

B.2.1 SULFATE AND MAGNESIUM ATTACK

Concrete degrades by sulfate and/or magnesium attack when sulfate or magnesium ions in the pore-fluid migrate into the concrete and react with the cement paste. Sulfate reacts with tri-calcium aluminate (C_3A) to form calcium aluminum sulfates leading to expansion and cracking of the surface of the concrete [Ref. B.1]. A related problem is the reaction of magnesium with the cement to form Brucite [$Mg(OH)_2$]. As the concrete cracks, its hydraulic conductivity increases, and water penetrates more easily into the interior, accelerating the deterioration of the concrete. Sulfate attack also results in a progressive loss of strength and mass due to deterioration in the cohesiveness of the cement hydration products. The reaction products have considerably greater volume than the reactants. This causes the expansion of the concrete which, in turn, results in cracking, spalling, and loss of strength. In addition, formation of gypsum causes a deterioration of the cement paste which results in a reduction in stiffness and strength, followed by more expansion, cracking, and loss of cohesiveness. Empirical studies indicate that the rate of attack by magnesium sulfate is twice that of sodium sulfate, and that the rate of attack is reduced by a low water-to-cement ratio and by low C_3A content. The rate of surface loss due to sulfate attack was calculated according to:

$$X = 0.55\, C_S\, (M_g^{2+} + SO_4^{2-})t$$

(Formula corrected to be consistent with Ref. B.1)

where

X	=	distance of corrosion into concrete (cm),
C_S	=	C_3A concentration in solid (mole/cm^3),
M_g^{2+}	=	Mg concentration in solution (mole/liter),
SO_4^{2-}	=	SO_4 concentration in solution (mole/liter), and
t	=	time (yrs).

The major sources of sulfate and magnesium at SRS are from weathering of rock minerals by rainfall. They are found in the groundwater at SRS. Concentrations of sulfate and magnesium in groundwater at SRS are very low. Sulfate concentrations range from 0.27 to 15 ppm (2.81×10^{-6} to 1.56×10^{-4} mol/L) with a mean and median of 3.66 and 2 ppm (3.81×10^{-5} and 2.08×10^{-5} mol/L), respectively. Magnesium concentrations range from 0.14 to 8 ppm (5.76×10^{-6} to 3.29×10^{-4} mol/L), with a mean and medium of

2.28 and 1.5 ppm (9.37×10^{-5} and 6.17×10^{-5} mol/L), respectively. The sum of Mg and SO_4 range from 0.57 to 18.5 ppm (1.51×10^{-5} to 3.77×10^{-4} mol/L) with a mean and median of 5.94 and 4.95 ppm (1.32×10^{-4} and 1.08×10^{-4} mol/L), respectively [Ref. B.2].

The amount of concrete damaged due to this sulfate attack was calculated to be:

- 0.03 cm in 10 years
- 0.34 cm in 100 years
- 3.4 cm in 1,000 years
- 34 cm in 10,000 years

B.2.2 CARBONATION

Carbonation occurs when calcium in concrete reacts with carbon dioxide (CO_2) to form calcium carbonate according to the following reaction.

$$Ca(OH)_2 + H_2O + CO_2 \Rightarrow CaCO_3 + 2H_2O).$$

At the E-Area disposal site, carbon dioxide will be present in soil-air and dissolved in soil-water. Carbon dioxide will slowly migrate into the concrete, potentially leading to a carbonated zone. Concrete degradation, in this case, is associated with concrete expansion due to corrosion of the reinforcement bars (i.e., rebar). Typically, the pH of concrete is very high which is favorable to very low rebar corrosion. However, the carbonation reaction can reduce the pore-fluid pH which, in turn, makes the rebar susceptible to corrosion.

Carbonation occurs most aggressively when the concrete is less than fully saturated with water, allowing CO_2 to diffuse through the air space in the concrete up to the reaction front within the concrete. This condition may exist on the inside of heated underground storage facilities. At the reaction front, CO_2 dissolves in pore water and combines with calcium to precipitate calcium carbonate. Reference B.1 shows that the depth of carbonation is proportional to the square root of time as shown in the equation below. The rate of carbonation depends on the moisture content of the concrete and its relative humidity, and ultimately on the type of cement used in the concrete mix.

Carbonation may also result in potentially beneficial effects. For example, carbonate carried by the pore-fluid into cracks and pores to the vault structure may precipitate and reduce the effective porosity of the vaults. At the bottom of the vault, water that has percolated through the vault roof will be saturated with portlandite $Ca(OH)_2$. The $Ca(OH)_2$ can react with soil-air containing CO_2, forming a calcium carbonate mass that then seals cracks and reduces effective pore sizes at any exposed surfaces of the vault structure.

Carbonation does not render the concrete less durable. Some fully-carbonated Roman concrete has survived to modern times. Shrinkage of the concrete may occur with carbonation as will a drop in the pH of the pore water. Carbonation of hydrated portland-cement pastes also results in reduced hydraulic conductivity and increased hardness. The pH shift can be from over 12 to about 8. At this lower pH. enhanced corrosion of steel reinforcement in the concrete may occur.

The rate of carbonation is dependent upon water saturation or relative humidity of the concrete. As relative humidity increases from 0 to 100%, the rate of carbonation passes through a maximum. Since water is required in the carbonation reaction, partially saturated conditions promote the reaction of CO_2 and $Ca(OH)_2$ to form $CaCO_3$; however, increasing the water content above that required for this reaction to proceed will slow the diffusion rate of CO_2 through the concrete and limit the carbonation reaction. Typical subsurface environments approach 100% relative humidity, resulting in a water-saturated concrete matrix. Therefore, slow rates of carbonation are commonly found. The following analytic expression was employed for estimating carbonation rate in the degradation model:

$$X = \left(2D_i \frac{C_{gw}}{C_g} t \right)^{1/2}$$

where,

X	=	depth of penetration of carbonation (cm),
D_i	=	intrinsic diffusion coefficient of Ca^{++} in concrete (cm^2/s),
C_{gw}	=	total inorganic carbon in groundwater or soil moisture ($mole/cm^3$),
C_g	=	$Ca(OH)_2$ bulk concentration in concrete solid ($mole/cm^3$), and
t	=	time (s).

Inherent in the use of this expression is the assumption that the concrete is water-saturated, and that the concrete is in direct contact with moisture containing a constant concentration of dissolved inorganic carbon. The effects of this carbonization were not provided directly but used in analysis of calcium hydroxide leaching and reinforcing steel corrosion, discussed in later portions of this appendix.

B.2.3 CALCIUM HYDROXIDE LEACHING

Where concrete is exposed to water, constituents in the concrete are leached. Alkalis are leached first, followed by calcium hydroxide. This process can be described in four stages:

1. Initially, the pH of standard concrete is approximately 13 due to the presence of alkali metal oxides and hydroxides. These alkali metals leach first.

2. After the alkali metals are leached, the pH is controlled at 12.5 by solid calcium hydroxide. Free (not bound by C-S-H gel) calcium hydroxide is leached first.

3. Following loss of free calcium hydroxide, calcium hydroxide is leached at a slower rate from the C-S-H gel. The C-S-H gel dissolves incongruously, while the pH drops to 10.5 and the calcium to silicon ratio drops to 0.85.

4. The pH is held to 10.5 by congruent dissolution of the C-S-H gel.

Ingress of water into the vaults and flow of water around the vaults will provide a pathway for leaching of soluble components from the concrete. In particular, leaching of calcium hydroxide from the concrete can lead to loss of strength [Ref. B.1]. Leaching is typically important in humid sites, such as the SRS, because high infiltration rates promote higher leaching rates.

The rate of leaching can be estimated using simple screening models or more complex numerical models. For this application, conservative screening calculations were performed. Two different simplifying assumptions were used in the calculations [Ref. B.3]: concrete-controlled leaching and geology-controlled leaching. Each is described below.

- Concrete-controlled leaching assumes that the leaching rate is limited by diffusion through the concrete into the surrounding soil. Once the calcium reaches the soil it is rapidly removed leading to a zero concentration boundary condition. If water is flowing around the vault, then a low concentration of calcium can conservatively be assumed in the soil moisture.

- For the case of geology-controlled leaching, diffusion of calcium into surrounding soils is assumed to limit the process. For this condition, the degradation effects are insignificant. This particular type of process is only valid in diffusion-dominated systems where water flow around the vault is low, such as beneath the vault or when infiltration is low.

The loss of calcium results in a decrease in strength of approximately 1.5% for every 1% loss of total calcium content. The rate of calcium hydroxide leaching depends primarily on the flow of water through the concrete, but also on diffusion into the surrounding geology, and diffusion across a reaction zone in the concrete. Advective transport of leached calcium hydroxide from the concrete structure will dominate only under high rates of groundwater flow, and preferential flow of groundwater through the structure.

Reference B.1 applied a shrinking core model to calcium hydroxide leaching. This model assumes that removal of calcium from the exterior of the concrete is rapid relative to movement of calcium through the concrete. Thus, leaching is controlled by conditions in the concrete and properties of the concrete, and so this process is referred to as "concrete-controlled leaching." As an alternative approach, Atkinson and Hearne also developed a leach model controlled by the surrounding geology ("geology-controlled leaching"). This model uses an equation for diffusion from a fixed concentration into a semi-infinite domain, with concentrations described by an error function [Ref. B.4] and allows for an analytic solution of the amount of calcium lost in a given amount of time. Both models predict that it will take over 1,000 years before calcium hydroxide leaching penetrates the upper 0.05 cm of the concrete. Both analytic models have been added to the degradation model. The equations used to approximate concrete-controlled and geology-controlled leaching, respectively, are:

$$X_C = \left(2D_i \frac{C_i - C_{gw}}{C_s} t\right)^{1/2}$$

and

$$X_G = 2\phi \frac{C_i - C_{gw}}{C_s} \left(\frac{R_d D_E t}{\pi}\right)^{1/2}$$

where,

X_c	=	depth of leach penetration due to concrete-controlled leaching (cm),
X_G	=	depth of leach penetration due to geology-controlled leaching (cm),
D_i	=	intrinsic diffusion coefficient of Ca^{++} in concrete (cm^2/s),
C_i	=	Ca^{++} concentration in concrete pore water ($mole/cm^3$),
C_{gw}	=	Ca^{++} concentration in ground/soil water ($mole/cm^3$),
C_s	=	bulk Ca^{++} concentration in concrete solid ($mole/cm^3$),
ø	=	porosity of soil (unitless),
R_d	=	retardation coefficient (unitless),
D_E	=	effective dispersivity/diffusivity of Ca^{++} in the surrounding geological material (cm^2/s), and
t	=	time in seconds.

A conservative estimate of the depth of leach penetration was obtained by summing X_C and X_G. Several typical calculations are given in Table B-1 for SRS soil conditions.

Table B-1. Calcium leaching from underground facilities.

Leaching time (years)	Leaching		
	Concrete-controlled	Geology-controlled	Total
10	0.24	0.03	0.27
100	0.75	0.26	1.01
1,000	2.4	2.7	5.1
10,000	7.5	27	34

B.2.4 CORROSION OF REINFORCING STEEL IN CONCRETE

Reinforcing steel (commonly called rebar) is used in concrete structures to increase tensile strength of the structure. Corrosion of the rebar is another possible mechanism of vault degradation. Corrosion occurs when iron in the rebar reacts with oxygen to form iron oxides. Corrosion of the rebar lowers its strength of the rebar and disrupts the integrity of the surrounding concrete. As the rebar corrodes, the tensile strength of the structure declines. For the E-Area Vaults, the structural role of the vault is essential to long-term isolation performance.

A reinforced-concrete structure may suffer structural damage due to the loss of the bond between steel and concrete. Corrosion of the rebar produces a reaction product of greater volume than the rebar. Since the concrete surrounding the reinforcement prevents free expansion, this expansion exerts pressure on the concrete, and thus causes cracking and potential spalling of the concrete structure, with consequent loss of strength. In the alkaline environment of standard concrete (low alkaline specialty concrete is used for the E-Area Vault construction), the rebar is protected from corrosion by the formation of a passivating layer around the rebar. This passivating layer, however, may be destroyed by the diffusion of chloride ions to the embedded steel (i.e., depassivation). Water-to-cement ratio and depth of concrete cover over the rebar are the most important factors in concrete construction that affect the time to depassivation. In the corrosion reaction, oxygen is electrochemically reduced and iron electrochemically oxidized, followed by conversion of the iron to iron oxides. The reaction rate is generally limited by diffusion of oxygen through the concrete to the rebar, with oxygen diffusion increasing over time as processes such as calcium hydroxide leaching and sulfate attack decrease the diffusion limiting concrete cover over the rebar.

As discussed previously, carbonation of the structure will occur too slowly to be a factor in concrete corrosion of the vaults. Accordingly, carbonation is even less of a factor in rebar corrosion. Concentrations of chloride ions in the soil moisture at the SRS are also too low to initiate active corrosion. To establish if rebar corrosion would significantly affect the rate of vault degradation, active corrosion was assumed to begin immediately after closure and no credit for the initiation lag time was taken in the corrosion calculations. Literature review of hydrogen evolution corrosion rates indicated a pH-dependence in the reaction rate. In the high pH range of typical concrete, the reaction rate is on the order of 1.5E-4 to 1E-5 cm/yr. If the pH drops below approximately 9, the reaction rate increases to values on the order of 1E-3 to 1E-4 cm/yr.

Corrosion of steel reinforcement results in a loss of strength due to loss of cross-sectional area of the rebar. Thus, the corrosion of reinforcing steel due to oxygen diffusion occurs in two steps. First, the passivating layer must be broken down before the onset of corrosion. The time to onset of corrosion was approximated by:

$$t_C = \frac{129 X_C^{1.22}}{WCR * Cl^{0.42}}$$

where,

t_c	=	time to onset of corrosion (yr),
X_c	=	thickness of concrete over rebar (inches),
WCR	=	water-cement ratio in concrete (kg/kg), and
Cl	=	chloride ion concentration in groundwater (ppm).

The reaction then proceeds, with a loss of reinforcing steel volume approximated by:

$$\%\text{Rebar Remaining} = 100\left(1 - \frac{4*9.4\left(\frac{cm^3}{mole}\right) s D_i C_S (t - t_C)}{\pi d^2 \Delta X}\right)$$

(Formula corrected to be consistent with Ref B.1)

where,

s	=	spacing between reinforcement bars (cm),
D_i	=	oxygen diffusion coefficient in concrete (cm^2/s),
C_{gw}	=	oxygen concentration in groundwater ($mole/cm^3$),
d	=	diameter of rebar (cm),
ΔX	=	depth of rebar below surface (in), and
C_s	=	bulk Ca^+ concentration in concrete solid ($moles/cm_3$).

Another mechanism of reinforcing steel corrosion is via the hydrogen evolution reaction. In this mechanism, H^+ ion from the water molecule is used as the source of oxidant for corrosion. H_2 is a by-product of this reaction. If we assume a low, constant rate of hydrogen evolution corrosion (i.e., a number from the low end of the literature range is adopted), then the relative volume of steel remaining is:

$$\frac{V_{H2}}{V_{ini}} = \frac{2at - d^2}{d^2}$$

where,

a	=	corrosion rate from hydrogen evolution reaction (cm/yr),
t	=	time (yr),
d	=	diameter of rebar (cm),
V_{H2}	=	volume of steel after H_2 corrosion, and
V_{ini}	=	initial volume of steel.

Reinforcement corrosion is typically modeled in two stages: (1) initiation and (2) active corrosion [Ref. B.1]. Initially the steel is protected from corrosion by a "passivating layer" of iron oxides on the metal surface. The stability of the passive layer is supported by the high pH of the concrete. Before significant corrosion can begin, the passive layer must be disrupted. This occurs when the pH of the

Once active corrosion begins, the corrosion rate may be limited by availability of oxygen. However, at very low oxygen concentrations, water can be used as a source of oxygen for corrosion (hydrogen evolution reaction). Because the thickness of concrete over the rear limits the availability of oxygen for rebar corrosion, hydrogen evolution was considered as an additional process for rebar corrosion. By combining the oxygen diffusion and hydrogen evolution reactions, an estimate of the total rebar corrosion can be made.

A bounding analysis for corrosion will be utilized by combining the rates due to oxygen-based corrosion and hydrogen evolution corrosion. The E-Area Vault structural analysis concluded that as the reinforcing steel corrodes, the roof and walls of the vault would crack due to excessive stresses which the corroded steel could not support. Their analysis assumed concrete cracks would occur at an assumed 40 ksi stress. Crack width and spacing were determined from spacing of the support reaching a maximum above the vertical support walls on the outside of the roof and a maximum on the lower side near the center of unsupported roof structure. Figure B-3 is illustrative of this condition. This condition allows water to leak into the structure from the resulting increased permeability of the concrete. The E-Area Vault analysis determined this hydraulic conductivity would decrease from 1×10^{-12} to 1×10^{-9} in 570 to 1,420 years [Ref. 3.1] depending upon vault design. During this time the reinforcing rod diameter had decreased about 16%.

Further analysis indicated that when the stress in the rebar reached 60 ksi, the yield strength of the steel, it will yield. Excess moment is then transmitted to other regions in the vault cell. The mid span region should reach yield strength first and then the excess moment is transferred to the region over the walls. When this rebar reaches its yield strength at all three locations, a "failure mechanism" is created. This allows the roof to sag and structural integrity to be lost. This is called roof collapse and would occur at 1,045 to 3,100 years [Ref. 3.1] depending upon the vault design.

B.2.5 VAULT INTERIORS

The degradation mechanisms that were considered for the walls and roof in contact with site soil are Mg + SO_4 attack, $Ca(OH)_2$ leaching, concrete carbonation, and oxic and anoxic corrosion of the re-bar. Several of these mechanisms will not operate under the conditions anticipated inside the vaults or will occur so slowly that their net effect over the life of the vaults will be insignificant. Only anoxic ("hydrogen evolution") corrosion is anticipated as a significant degradation process originating inside the vault, as discussed below. The above description will probably also apply to the YM EIS Underground facilities until roof collapse.

Magnesium and sulfate attack requires a source of dissolved Mg and SO_4 in accordance with the concrete such as would be provided by a moist soil. No continuous source of Mg and SO_4 contacts the concrete in the vault interior, so this mechanism is not anticipated to operate.

Two forms of calcium hydroxide leaching, concrete-controlled and geology-controlled, were considered. The concrete-controlled leaching mechanism assumed a zero-concentration boundary condition at the surface of the concrete, a condition which would require groundwater to flow over the concrete surface and "sweep" the calcium away from the surface as it diffuses out of the concrete. Inside the vaults, during the period of performance prior to collapse, there is no recognizable mechanism to create this zero-concentration boundary. As a result, a chemical diffusion gradient from the interior of the concrete towards the concrete surface will not be established and diffusion will not occur.

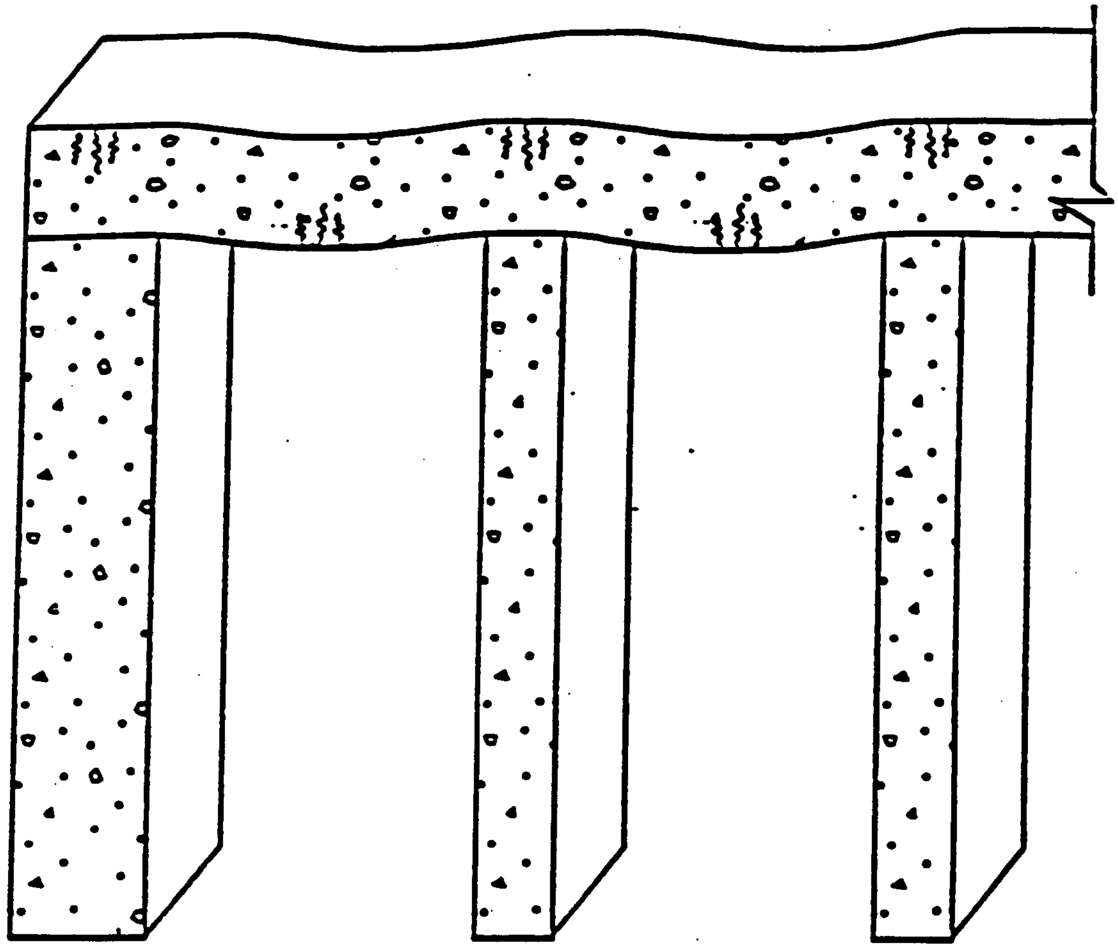

NOT TO SCALE
DEFLECTION HAS BEEN EXAGGERATED FOR EMPHASIS

Figure B-3. Low Activity Waste Vault concrete cracking in critical stress regions.

Geology-controlled leaching assumes that a concentration gradient can be established into the (soil) material adjacent to the concrete. This is physically impossible in the LAW vault because of the lack of in-filling material. For ILT and ILNT vaults, where cement grout will contact the walls, the calcium concentration in the grout porewater will be identical to that in the concrete at all times. These conditions prevent a concentration gradient from forming outwards away from the concrete.

Concrete carbonation occurs in the presence of dissolved carbonate and calcium in the porewater of the concrete. Leaching of calcium hydroxide provides a source of calcium and diffusion of carbonate ion from soil and water in contact with the concrete, which provides a source of carbonate. The carbonate in the soil and water is replenished from dissolution of CO_2 gas from soil and air. Inside the LAW vault, the air space will contain CO_2, although most likely at concentrations much less than in a biologically-active soil; differences of one to two orders of magnitude would be a reasonable estimate. Carbonation would most likely occur, however, with only atmospheric levels of CO_2 driving the reaction; the carbonation front would advance at a much slower rate than for the outer surfaces of the vaults. From the empirical relationship that was used to describe carbonation, a slowing of the movement of the carbonation front by an order of magnitude would be possible.

Corrosion of the reinforcing bar in concrete under oxygenated conditions requires an initial depassivation of the steel surface. The mechanism that has been invoked in our modeling relies on diffusion of chloride to the passivating layer. Depassivation is followed by oxidation of the exposed steel. The interior of the vaults does not provide a source of chloride for the depassivation mechanism. Degradation modeling of the interior of the vaults should therefore not include oxic corrosion of rebar, unless the concrete mix is such that the pH of the concrete is below 9.

Anoxic corrosion of rebar will occur in the presence of moisture in the concrete. Since water-saturated concrete has been assumed for degradation modeling, this mechanism would proceed at a rate approximately the same as for the exterior surfaces of the vault. Adjustments to the rate caused by a decrease in pH at the corroding surface following carbonation of the local concrete will not be required.

In summary, the dominant degradation mechanism for the interior surface of the vaults will likely be anoxic corrosion of re-bar. Carbonation is also likely to occur; however, the rate of advance of the carbonation front will be significantly less than for exterior surfaces. The effect of carbonation on anoxic corrosion will likely not be an important consideration.

B.3 Appendix B References

B.1 Walton, J. C., L. E. Pansky, and R. W. Smith, 1990, *Models for Estimation of Service Life of Concrete Barriers in Low-Level Radioactive Waste Disposal*, NUREG/CR-5542, EGG-2597, U.S. Regulatory Commission, Washington, D.C.

B.2 Marine, I. W., 1976, *Geochemistry of Groundwater at Savannah River Plant*, DP-1356, E. I. DuPont de Nemours and Co., Savannah River Laboratory, Aiken, South Carolina.

B.3 Atkinson, A. and Hearne, 1984, *An Assessment of the Long-Term Durability of Concrete in Radioactive Waste Repositories*, AERE-R11465, Harwell, England.

B.4 Crank, J., 1975, *Mathematics of Diffusion*, Oxford University Press, Oxford, England.